http://dx.doi.org/10.5935/0103-5053.20150328

J. Braz. Chem. Soc., Vol. 26, No. 12, 2471-2495, 2015.
Printed in Brazil - ©2015 Sociedade Brasileira de Química
0103 - 5053 $6.00+0.00

Review

From Lighting to Photoprotection: Fundamentals and Applications of Rare Earth Materials

Paulo C. de Sousa Filho,[a,#] Juliana F. Lima[a,b] and Osvaldo A. Serra*[,a]

[a]*Departamento de Química, Faculdade de Filosofia, Ciências e Letras de Ribeirão Preto, Universidade de São Paulo, Av. Bandeirantes, 3900, 14040-901 Ribeirão Preto-SP, Brazil*

[b]*Departamento de Química Geral e Inorgânica, Instituto de Química, Universidade do Estado do Rio de Janeiro, R. São Francisco Xavier, 524, 20550-900 Rio de Janeiro-RJ, Brazil*

Light and rare earths (RE) have a long lived relationship that dates from the discoveries of these elements in the nineteenth century. Since then, the increasing comprehension of their spectroscopic properties conducted to a wide and alluring literature about light absorption and emission by this particular and fascinating group. For more than 50 years, RE-containing solid-state optical materials have undoubtfully been an important subject for the development of more efficient lighting, visualization, communication and health everyday applications. Therefore, this review introduces the spectroscopic properties of rare earth materials and their applications, with a brief discussion of the main mechanisms of light absorption and emission from a 4f elements inorganic physical chemistry perspective. Special attention is devoted to the use of these elements in systems concerning photoprotection and to the fundamentals of visible light generation for lighting and visualization.

Keywords: rare earths, lanthanoids, spectroscopy, luminescence, photoprotection, phosphors

1. Introduction

In the ca. 100 years that followed the discovery of yttrium by Gadolin in 1794, rare earth (RE) elements were considered as mere laboratory curiosities with a limited practical importance.[1-6] Nevertheless, throughout the twentieth century, the improvement of separation procedures enabled the obtainment of larger amounts of RE with increased purity, which lead to the development of countless high technology applications.[3,4,7-10] In the last years, this group of seventeen chemically similar elements (Sc,Y, and the lanthanoids, La-Lu)[11,12] has definitively left the bottom of periodic tables and chemistry textbooks to figure both in the most up-to-date research subjects and in the geopolitical scenario around the world. Currently, RE elements can be associated with practically all everyday activities of modern society due to their enormously wide range of applications, which comprise materials for catalysis, magnets, phosphors, ceramics, polishing, glasses, batteries, among others.[1-5] RE elements play a central role in the so-called green policies worldwide,[13,14] since they are strictly associated with several key points of environmentally sustainable economic growth, such as (*i*) clean energy generation (magnets for wind turbines[15,16] and photovoltaic systems for solar panels),[17,18] (*ii*) more efficient energy storage and conversion (rechargeable NiMH batteries for hybrid vehicles[19,20] and high-output phosphors for lamps and displays),[21-24] (*iii*) reduction of pollution indices (catalytic converters for engine exhausts[25-28] and (photo)catalysts for degradation of harmful waste),[29,30] and (*iv*) optimization of petroleum resources (cracking catalysts).[31] Therefore, the availability of these elements is considered to be an important bottleneck for the development and application of new technologies, which since 2009 has caused an increasing concern regarding their supply, as the RE global market is dominated by China.[32] This, in turn, stimulates the search for alternative sources of RE elements notably by means of recycling of waste products in the so-called "urban mining",[33-35] whereas cleaner approaches for the RE mining and metallurgy are also required.[36,37]

*e-mail: osaserra@usp.br
[#]On the leave of absence from Departmento de Química, Faculdade de Filosofia, Ciências e Letras de Ribeirão Preto, Universidade de São Paulo. Current address: Solid State Chemistry Group, Laboratoire de Physique de la Matière Condensée, Ecole Polytechnique, Université Paris-Saclay, Route de Saclay 91128 Palaiseau, France.

This critical dependence of advanced technologies upon REs is particularly more evident in the field of optical materials,[38-43] since these elements are almost irreplaceable for a number of specific functions comprising absorption or emission of electromagnetic radiation. Such applications range from optical devices technologies[21-24] (e.g., lasers, lamps) to health[44-47] (e.g., UV protection, biological markers). This is only possible due to the unique spectroscopic properties of the lanthanoids, which currently consists in a highly significant topic in chemistry, physics and materials science. The obtainment of solid state RE-based materials and the description of their interaction with the electromagnetic radiation are thereby crucial for the comprehension of their activity mechanisms and for the improvement of their functionalities in different light-emitting/absorbing systems.

In summary, light and the rare earths are intimately related since the discoveries of these elements in the nineteenth century[3,4] and, after the 1960s, RE-containing solid state optical materials are an undoubtfully important subject for the development of more efficient lighting, visualization, communication and everyday health applications. In this regard, the literature is considerably rich in papers detailing the synthesis and the application of optical properties associated with RE ions, which normally requires a quite specific focus on particularly desired systems due to the broadness of this field. Therefore, in the context of the International Year of Light (IYL 2015), this review presents an introduction to the spectroscopic properties of rare earth elements and their application in solid state optical devices, with a brief discussion of the main mechanisms of light absorption and emission from a perspective of 4f elements inorganic physical chemistry. Special attention is devoted to the use of these elements in systems concerning photoprotection, particularly against sunlight and UV radiation, and to the fundamentals of the application of RE materials in the generation of visible light for lighting and visualization.

2. Rare Earths: General Properties and Electronic Structure

The chemistry of rare earths is characterized by the trivalent state and by a high similarity among their chemical behaviors. This, for instance, means that REs always occur as mixtures in nature and leads to a remarkably difficult separation of these elements.[5,10,48] However, this group displays several differences in comparison to main group elements as a consequence of the filling of 4f orbitals in the case of lanthanoids.[4] In this sense, Sc, Y and Lu are usually considered to belong to group 3 of the periodic table (as well as Lr), while La-Yb (and Ac-No) are considered to comprise the f-block elements.[3,49-51] The tendency to form trivalent ions, as well as low reduction potentials and low electronegativities ascribed to REs is determined by their electron configurations. In the case of trivalent lanthanoids (Ln^{3+}), electron configurations assume the form [Xe] $4f^n$ (n = 0-14), in which the xenon core displays $5s^2$ and $5p^6$ filled orbitals that are radially more external than 4f orbitals. This, in turn, results in a low interaction of 4f electrons with the chemical environment, which culminates in a low degree of covalence in their chemical bonds and in a high similarity in chemical properties. These ions interact with ligands predominantly through ionic or ion-dipole bonds, thus behaving as hard acids in the Pearson HSAB classification. Another main characteristic associated with lanthanoids is the termed "lanthanoid contraction", which consists in the progressive reduction of atomic and ionic radii from La to Lu. This characteristic is mostly due to a large increase in the effective positive charge over $5s^2$ and $5p^6$ electrons with increasing atomic numbers, as an effect of the low shielding power of 4f electrons. Additionally, ca. 10% of the lanthanoid contraction is usually ascribed to relativistic effects due to the high atomic numbers of these elements.[52-54] The lanthanoid contraction accounts for the decrease of basicity of Ln^{3+} ions along the series and results in very subtle differences in solubility and crystal structures of their compounds. The most remarkable chemical differences within the lanthanoids take place when divalent or tetravalent ions can be formed, which was one of the most important approaches for RE purification prior to the development of ion exchange[55-57] and solvent extraction[10,48] techniques. In most of the lanthanoids, the fourth ionization energy is higher than the sum of the three first ionization energies, thus making trivalent ions highly stable with respect to oxidation. Cerium, praseodymium and terbium form stable tetravalent species, from which only Ce^{4+} can exist in aqueous solution. Ions with high third ionization energies (Sm, Eu, Tm, Yb) can form stable divalent species, which normally are strongly reducing agents that are readily reoxidized in aqueous solutions.[1-6]

Despite the fact that the [Xe] $4f^n$ electron configurations introduce highly similar chemical properties, progressive filling of 4f orbitals results in particular physical properties with respect to the spectroscopy and magnetism of lanthanoid ions. Spectroscopic properties of Ln^{3+} ions are governed by the shielding effect of $5s^2$ and $5p^6$ electrons over 4f electrons, which gives rise to well-defined energy levels. As a consequence, electronic structures of lanthanoids are unique among the elements, since similar behavior cannot be observed in other groups, not even within actinoids (5f). In this sense, spectrochemical descriptions of Ln^{3+} ions mostly

comprise the evaluation of energy levels arising from $4f^n$ configurations, where the number of states can be very high (Table 1). Due to the shielding effect of [Xe] core outmost electrons, the weak interactions of 4f electrons with ligands result in negligible effects regarding coordination geometries and enable the description of their electronic properties in terms of the crystal field theory. $4f^n$ configurations can in a first approach be characterized by the three quantum numbers of angular momentum, namely total spin angular momentum (S), total orbital angular momentum (L), and total angular momentum (J), in which the spin-orbit coupling (LS) is assumed to obey the Russell-Sauders scheme. In free ions, energy levels are first affected by the central field (H_0), which can be considered as the hydrogenoid fraction of the level approximation. The central field depends on the principal and azimuthal quantum numbers and separates the different configurations (5p, 4f, 5d, etc.) in ca. 10^5 cm^{-1} in energy. Since the H_0 term has a purely radial contribution and, consequently, a spherical symmetry, the degeneracy of 4f configurations is not removed by the central field. However, the interelectronic repulsion interaction ($H_{e\text{-}e}$) that is inherent to multielectronic systems removes the degeneracy of 4f configurations. As a result, low multiplicity $^{(2S+1)}L$ levels have lower energies and are separated from higher energy levels by ca. 10^4 cm^{-1}. Each of these levels is further affected by the spin-orbit coupling term (H_{SO}), which removes the degeneracy of $^{(2S+1)}L$ levels with respect to their 2S + 1 components of total angular momentum, resulting in a typical separation of 10^3 cm^{-1} within the $^{(2S+1)}L_J$ levels. Finally, as also observed in d electrons, diminution of the symmetry from a spherical field (free ion) to a non-spherical crystal field (V_{CF}) results in the loss of degeneracy of $^{(2S+1)}L_J$ levels, which can split into a maximum of 2J + 1 Stark components according to the crystal field symmetry, with energy separations of ca. 10^2 cm^{-1}.

As the nature of the crystal field has a low effect on the final energies of $^{(2S+1)}L_J$ levels, basic properties regarding 4f configurations can be represented for each trivalent lanthanoid in a practically universal scheme applicable to any chemical environment, which is known as the Dieke diagram (Figure 2). This diagram has been experimentally extended up to ca. 70,000 cm^{-1}, whereas theoretical determinations enable the description of 4f configurations up to ca. 200,000 cm^{-1}. Trivalent ions of lanthanum and lutetium have closed configurations and are not represented in the diagram. These ions, as well as Sc^{3+} and Y^{3+}, have $^1S_0$ ground terms and cannot display electron transitions within the 4f configuration. Consequently, they are considered as spectroscopically inert ions, thus being mostly applied in the composition of host lattices as further discussed. With regard to the other trivalent lanthanoids, ground terms change from a doublet to an octet from Ce^{3+} to Gd^{3+} (Table 1), whereas from Tb^{3+} to Yb^{3+} ions assume equivalent terms in the opposite order, according to the

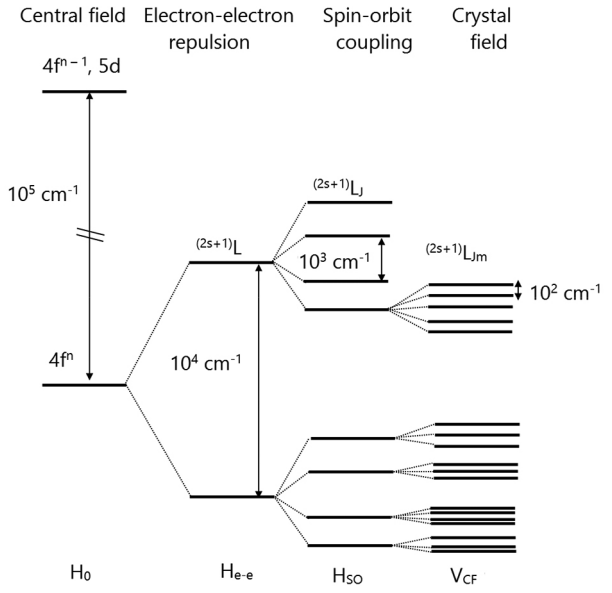

Figure 1. Schematization of the perturbations that remove the degeneracy of $4f^n$ configurations giving rise to their corresponding states.

Table 1. Ground levels and number of states arising from $4f^n$ configurations, with examples of their corresponding lanthanoid ions

$4f^n$	Example	Ground level	$4f^n$	Example	Ground level	Number of levels	Number of microstates
$4f^0$	La^{3+},Ce^{4+}	$^1S_0$	$4f^{14}$	Lu^{3+},Yb^{2+}	$^1S_0$	1	1
$4f^1$	Ce^{3+},Pr^{4+}	$^2F_{5/2}$	$4f^{13}$	Yb^{3+},Tm^{2+}	$^2F_{7/2}$	2	14
$4f^2$	Pr^{3+}	$^3H_4$	$4f^{12}$	Tm^{3+}	$^3H_6$	13	91
$4f^3$	Nd^{3+}	$^4I_{9/2}$	$4f^{11}$	Er^{3+}	$^4I_{15/2}$	41	364
$4f^4$	Pm^{3+}	$^5I_4$	$4f^{10}$	Ho^{3+}	$^5I_8$	107	1001
$4f^5$	Sm^{3+}	$^6H_{5/2}$	$4f^9$	Dy^{3+}	$^6H_{15/2}$	198	2002
$4f^6$	Eu^{3+},Sm^{2+}	$^7F_0$	$4f^8$	Tb^{3+},Dy^{4+}	$^7F_6$	295	3003
$4f^7$	Gd^{3+}, Tb^{4+}, Eu^{2+}	$^8S_{7/2}$	–	–	–	327	3432

Table 2. Description of the perturbations affecting the energy levels of $4f^n$ configurations in lanthanoid ions

Interaction	Description	Expression	Energy splitting / cm^{-1}	Analysis
H_0 (central field)	elecrons in the field of the nucleus (hydrogenoid fraction)	$-\left(\frac{h^2}{2m_e}\sum_{i=1}^{i=N}\nabla_1^2+\sum_{i=1}^{i=N}\frac{ze^2}{r_i}\right)$	10^5	UV or VUV absorption spectroscopy
$H_{e\text{-}e}$ (multielectron repulsion)	mutual repulsion between electrons	$+\sum_{i<j}^{N}\frac{ze^2}{r_{ij}}$	10^4	UV-Vis absorption or luminescence spectroscopy
H_{SO} (spin-orbit coupling)	combination of spin and orbital angular momenta	$+\sum_{i=1}^{i=N}\xi(r_i)(s_i,l_i)$	10^3	
V_{CF} (crystal field)	electric field due to the electrons of ligand atoms, comprising the expansion of crystal field parameters with regard to spheric harmonics	$+\sum_{kq}A_{kq}\sum_i r_i^k Y_{kq}(\upsilon_i,\varphi_i)$	10^2	UV-Vis or NIR absorption/ luminescence spectroscopy or laser site selective spectroscopy

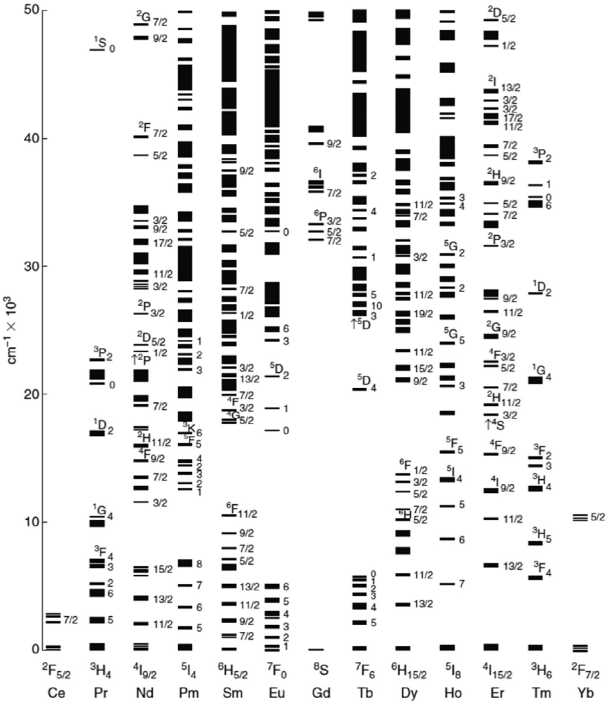

Figure 2. Energy levels of the $4f^n$ configurations of trivalent lanthanoids (Ln^{3+}). Adapted from references 40 and 41.

electron-hole formalism. However, ground levels in ions with configurations from $4f^8$ to $4f^{13}$ correspond to terms with the highest J = L + S value.

3. Light Emission and Absorption by Lanthanoid Ions: Basic Aspects

3.1. Selection rules

As atomic orbitals represent wavefunctions that are solutions of the Schrödinger equation in an electronic system, such functions must be orthogonal if they represent non-degenerate states, which is known as the Hermitian condition. Therefore, wavefunctions of different electronic states *a* and *b* of a particular electronic configuration, represented by Ψ_a and Ψ_b, the condition $\int\Psi_a\Psi_b d\tau = 0$, where $d\tau$ represents all coordinates of the system, must be obeyed. If this integral assumes a non-zero value due to a perturbation operating over the two non-degenerate electronic states, then a photon can be absorbed or emitted by the system, which will undergo a transition from the *a* state to the *b* state. Such a transition will be possible if a resonance condition is obeyed, since the energy of the emitted or absorbed photon must be equal to the difference between the energies of the *a* and *b* states. Nevertheless, only perturbations that fulfill some specific requirements can lead to a transition between these electronic states. Such conditions are summarized by the so-called selection rules, which arise from the condition that the integral $\int\Psi_a^*\mu\Psi_b d\tau$ must be non-zero. In this case, "*" represents the complex conjugate of the wavefucntion and μ is the operator related to the perturbation over the system. This perturbation can be considered as a result of the interaction of the system with electric or magnetic components of the electromagnetic radiation oscillating field. The term μ is thereby defined as a transition momentum operator. Selection rules are, in a broad sense, conservation laws applied to angular momenta and parities of photon and atomic/molecular wavefunctions. The integral $\int\Psi_a^*\mu\Psi_b d\tau$ is usually represented as a Dirac notation: $\langle a|\mu|b\rangle$, in which $|b\rangle$ denotes the wavefunction of the b state and $\langle a|$ represents the complex conjugate of the a state. If the integral vanishes, then the process is classified as a forbidden transition, which means that the process has a low probability to occur.

Electronic transitions can thereby be defined in terms of the nature of transition momentum operators. Differences between electric and magnetic transitions

arise from the angular momentum of photons involved in each case. Photons are fundamental particles that obey the Bose-Einstein statistics (bosons), thus being associated with a unitary spin ($s_\gamma = 1$) and an intrinsic odd parity ($\pi_\gamma = -1$). Due to their relativistic nature, photons must have a zero rest mass, and their spin (s_γ) and angular momentum (l_γ) quantum numbers are not independent, since a photon cannot have a zero total angular momentum ($j_\gamma \geq 1$). The most common physical situation in light-matter interactions consists in the absorption or emission of a photon with a zero orbital angular momentum ($l_\gamma = 0$). In this case, the total angular momentum of the photon arises from its spin, then $s_\gamma = 1$, $l_\gamma = 0$, and $j_\gamma = 1$, while the intrinsic odd parity ($\pi_\gamma = -1$) is unchanged. An electronic transition involving a photon with such characteristics comprises an interaction with the electric component of the radiation, thus being described as an electric dipole transition.

However, a photon involved in the absorption or emission process can also display a unitary orbital angular momentum ($l_\gamma = 1$), which results in an alteration to an even parity state ($\pi_\gamma = 1$). The combination of the non-zero orbital angular momentum of such a photon with its spin ($s_\gamma = 1$) results in two possible total angular momentum states, namely $j_\gamma = 1$, and $j_\gamma = 2$ ($j_\gamma = 0$ is not possible for a photon). If this photon with $l_\gamma = 1$ is characterized by a unitary total angular momentum ($j_\gamma = 1$), the electronic transition associated to the process is determined by an interaction with the magnetic component of the radiation, thus being termed as a magnetic dipole transition. If a photon with $l_\gamma = 1$ carries a total angular momentum of 2 ($j_\gamma = 2$), the transition is associated with the electric component of the radiation, thereby being called as a electric quadrupole transition (Table 3). Although possible, processes with $j_\gamma = 2, 3, n$, etc. (quadrupole, octupole, 2^n-pole, etc.) have a much lower probability than dipole transitions and usually display a low contribution to electronic spectra.

In all these possible electronic transitions, conservation laws impose that alterations of parity and angular momentum must be compensated by the parity and angular momentum of the photon involved in the photophysical event. Therefore, in an emission process, for instance, the parity and the angular momentum of the initial electronic state must be the same as the combined angular momenta and parities of the photon and final electronic state. With respect to the angular momentum, which is an additive property, evaluation of the transition probability is facilitated through the use of $^{(2S+1)}L_J$ spectroscopic term symbols. In both electric and magnetic dipole transitions, as the photon carries an angular momentum of $j_\gamma = 1$, the alteration in J introduced by the electronic transition must be $\Delta J = 0, \pm 1$, where a $J = 0 \leftrightarrow 0$ transition is not allowed. As the electric component of the electromagnetic radiation does not operate over spin components of electronic wavefunctions, electric dipole transitions must not lead to spin changes in the involved states. This spin conservation rule for electric dipole transitions ($\Delta S = 0$)

Table 3. Photon properties and selection rules of different electric and magnetic transitions between generic *a* and *b* electronic states represented by $^{(2S+1)}L_J$ terms

Nature of the interaction		Photon total angular momentum	Photon parity	Selection rules
Electric				
	dipole	$j_\gamma = 1$	$\pi_\gamma = -1$	$\Delta J = 0, \pm 1$ (except $J = 0 \leftrightarrow 0$) $\Delta S = 0$, $\Delta L = 0, \pm 1$, (except $L = 0 \leftrightarrow 0$) $\Delta \ell = \pm 1$ $\pi_a = -\pi_b$
	quadrupole	$j_\gamma = 2$	$\pi_\gamma = +1$	$\Delta J = 0, \pm 1, \pm 2$ (except $J = 0 \leftrightarrow 0,1$ and $½ \leftrightarrow ½$) $\Delta S = 0$, $\Delta L = 0, \pm 1, \pm 2$ (except $L = 0 \leftrightarrow 0$) $\Delta \ell = 0, \pm 2$ $\pi_a = \pi_b$
	2^n-pole	$j_\gamma = n$	$\pi_\gamma = (-1)^n$	depends on n
Magnetic				
	dipole	$j_\gamma = 1$	$\pi_\gamma = +1$	$\Delta J = 0, \pm 1$ (except $J = 0 \leftrightarrow 0$) $\Delta S = 0, \pm 1$ $\Delta L = 0, \pm 1$ $\Delta \ell = 0$ $\pi_a = \pi_b$
	quadrupole	$j_\gamma = 2$	$\pi_\gamma = -1$	$\Delta J = 0, \pm 1, \pm 2$ (except $J = 0 \leftrightarrow 0,1$ and $½ \leftrightarrow ½$) $\Delta S = 0 \pm 1$, $\Delta L = 0, \pm 1$ (except $L = 0 \leftrightarrow 0$) $\Delta \ell = \pm 1$ $\pi_a = -\pi_b$
	2^n-pole	$j_\gamma = n$	$\pi_\gamma = (-1)^{n-1}$	depends on n

therefore imposes that the alteration in the total angular momentum must be associated with an alteration of ±1 in the orbital angular momentum, which is written as $\Delta L = 0, \pm 1$ (where $L = 0 \leftrightarrow 0$ is not allowed). Regarding the parity, which is a multiplicative property, the evaluation can be simplified by the group theory description of $\int \Psi_a^* \mu \Psi_b d\tau$, where this integral will be non-zero only if the direct product of the symmetry representations of the initial and final states and transition momentum contain the totally symmetric representation of the system point group. These representations have even parities, which are denoted by "g" in point groups with inversion center. As mentioned above, photons have an odd parity ($\pi_\gamma = -1$, represented by "u") in electric dipole transitions and so does the transition operators in these cases. The direct product related to the $\int \Psi_a^* \mu \Psi_b d\tau$ integral will be even (g) only if the initial and final states display opposite parities ($u \times u \times g = g$ or $g \times u \times u = g$). An electric dipole transition will be allowed if there is a change in the parity in the involved electronic states ($\pi_a = -\pi_b$). This restriction is commonly known as the Laporte rule, which imposes the limitation that $\Delta \ell = \pm 1$ to electric dipole transitions in order to fulfill the parity requirements, where ℓ is the azimuthal quantum number of the considered electronic states (Table 3).

In magnetic dipole transitions, photons have both spin and angular momenta, as well as an even parity ($\pi_\gamma = +1$), so that the transition operator has a g symmetry. In fact, the magnetic dipole momentum operator transforms as rotations over the x, y, and z axes, thus being related to the R_x, R_y, and R_z functions in character tables. As a result, in a magnetic dipole transition, the direct product will be even only if the initial and final states have the same parity ($g \times g \times g = g$ and $u \times g \times u = g$). Such a transition does not necessarily conduct to an alteration in the orbital angular momentum ($\Delta \ell = 0$ and $\Delta L = 0 \pm 1$). Moreover, in contrast to electric dipole transitions, the magnetic component of the electromagnetic radiation is expected to effectively interact with the electron spin. Therefore, in this case, the alteration in the total angular momentum can also arise from the spin, so $\Delta S = 0 \pm 1$ is a possible condition for magnetic dipole transitions (Table 3).

3.2. f-f transitions

The classical selection rules are normally strictly valid only for light elements, although their basis can be applied for more complicated schemes. In the case of RE ions, the Russell-Saunders coupling is not a good approximation, since high atomic numbers induce a decrease in electrostatic interactions and an increase in the importance of spin-orbit interactions. As a result, spin-orbit interactions have almost the same magnitude of the electrostatic interactions in RE^{3+} ions (Figure 1, Table 2), which makes L and S no longer good quantum numbers. In this sense, although J continues as a good quantum number, the notation $^{(2S+1)}L_J$ of a particular state of a $4f^n$ configuration becomes a simple indication of dominant components of spin and orbital angular momentum and term symbols cannot be strictly considered to account for selection rules. Therefore, an intermediate coupling scheme is required for describing free ion 4f states, in which 4f wavefunctions are expanded in linear combinations of different Russel-Saunders states.[43,58,59] Consequently, a particular state denoted as $^{(2S+1)}L_J$ actually corresponds to a linear combination of different terms with the same J value.

Considering the fundamental selection rules, transitions within different levels of $4f^n$ configurations by an electric dipole mechanism are forbidden by parity and, in several cases, by spin. This accounts for the low molar absorptivity coefficients that are normally observed in trivalent lanthanoids. However, as reported in the classic work of van Vleck,[60] several f-f transitions display intensities that are largely higher than expected for forbidden transitions, even considering the results of intermediate coupling scheme for the relaxation of some selection rules. Indeed, at that time, a number of authors observed that f-f intensities were also higher than expected for magnetic dipole-allowed, electric quadrupole-allowed, and vibronically relaxed electric dipole transitions in some lanthanoid compounds.

In 1962, Judd[61] and Ofelt[62] independently proposed that f-f transitions occur through a forced electric dipole mechanism. These two publications consisted in one of the main advances in the comprehension of 4f transitions and still today are considered as landmark papers of electronic spectroscopy.[63,64] In addition, as mentioned by Prof Brian G. Wybourne, "… the coincidence of discovery was indicative that the time was right for the solution of the problem."[65] The termed Judd-Ofelt theory describes the intensities of 4f transitions in solids and solutions by considering the chemical environment around the central ion as a static perturbation of the free ion, whereas interactions between electrons of different configurations are neglected. For the accurate treatments of the Judd-Ofelt theory, readers are referred to a more specific literature.[63,66,67]

The Judd-Ofelt theory is based in a crystal field conception, where ligands are considered as point charges that do not introduce covalence in chemical bonds of Ln^{3+} ions, which are considered to be embedded in an optically isotropic medium. The crystal field potential (V_{CF}) is then considered as a perturbation that mixes the terms of $4f^n$ configurations with high energy terms of opposite parity (as 5d or 5g, for instance). In this sense, two wavefunctions

Ψ_a and Ψ_b arising from a $4f^n$ configuration will assume a mixed parity state due to the crystal field perturbation, as described in equation 1.

$$\langle \Psi_a | = \langle \varphi_a | + \sum_\beta \frac{\langle \varphi_a | V_{CF} | \varphi_\beta \rangle}{E_a - E_\beta} \langle \varphi_\beta |, \text{ and}$$

$$| \Psi_b \rangle = | \varphi_b \rangle + \sum_\beta \frac{\langle \varphi_b | V_{CF} | \varphi_\beta \rangle}{E_b - E_\beta} | \varphi_\beta \rangle. \quad (1)$$

In equation 1, φ_a and φ_b are same parity states, as two levels of a $4f^n$ configuration for instance; φ_β is an opposite parity state, as a $4f^{n-1}$ 5d configuration; and E_a, E_b and E_β are the energies associated with each of these states. In this case, an electric dipole transition between *a* and *b* states related to a μ_{ED} operator will be governed by the integral:

$$\langle \Psi_a | \mu_{ED} | \Psi_b \rangle = \sum_\beta \left[\frac{\langle \varphi_a | V_{CF} | \varphi_\beta \rangle \langle \varphi_\beta | \mu_{ED} | \varphi_b \rangle}{(E_a - E_\beta)} + \frac{\langle \varphi_a | \mu_{ED} | \varphi_\beta \rangle \langle \varphi_\beta | V_{CF} | \varphi_b \rangle}{(E_b - E_\beta)} \right]. \quad (2)$$

The crystal field enables the integral in equation 2 to be non-zero for an electric dipole transition even though the φ_a and φ_b states have the same parity, since this perturbation provides a non-negligible mixing with the opposite parity φ_β state. These assumptions are the basis of the approaches of Judd and Ofelt, which also considered the odd part of the crystal field as a perturbation that mixes the opposite parity states. Such transition scheme induced by the crystal field perturbation is commonly known as forced (or induced) electric dipole mechanism. Further assumptions of this treatment comprise the consideration that φ_β opposite parity states are degenerate in J and have a sufficiently high energy separation from the same parity states, in order that $(E_a - E_\beta)$ is close to $(E_b - E_\beta)$ is a good approximation. Based in these considerations, Judd and Ofelt took advantage of the solid algebraic methods developed by Giulio Racah in his four seminal papers some years before[68-71] to propose an expression that relates two arbitrary $\langle 4f^n \Psi J|$ states through the electric dipole momentum operator μ_{ED}. The achievement of this relation was also largely helped by computers that have been developed at the end of the 1950s, which allowed the tabulation of all angular momentum coupling coefficients.[67] The simplified form of this relation is given by equation 3, which summarizes the correlation between 4f states and the electric dipole operator:

$$\left| \langle \Psi' J' | \mu_{ED} | \Psi J \rangle \right|^2 = \frac{1}{2J+1} \sum_\lambda \Omega_\lambda \langle \Psi' J' \| U^{(\lambda)} \| \Psi J \rangle, \quad (3)$$

where the term $\langle \Psi' J' \| U^{(\lambda)} \| \Psi J \rangle$ is the reduced matrix element of the J $\leftrightarrow$ J' transition. The Ω_λ (λ = 2, 4, 6) terms are known as Judd-Ofelt intensity parameters. Such phenomenological parameters, usually expressed in cm^2, depend on radial wavefunctions of the $4f^n$ configuration, admixing opposite parity states ($4f^{n-1}$ 5d, $4f^{n-1}$ 5g), and crystal field parameters. Therefore, the Ω_λ parameters can be considered as a combination of intrinsic properties of the RE ion and characteristics of the chemical environment. The Ω_λ terms are adjustable parameters that can be applied for the theoretical calculations of the 4f intensities, whereas they are usually calculated from absorption or emission spectrum for different coordination environments. The Ω_λ parameters can be directly related to dipole strengths (D_{ED}) of forced electric dipole transitions in $4f^n$ configurations, as shown in equation 4:

$$D_{ED} = e^2 \sum_{\lambda=2,4,6} \Omega_\lambda \left| \langle \Psi' J' \| U^{(\lambda)} \| \Psi J \rangle \right|^2, \quad (4)$$

where e is the elementary charge (4.803×10^{-10} esu) and $\left| \langle \Psi' J' \| U^{(\lambda)} \| \Psi J \rangle \right|^2$ are the tabulated square reduced matrix elements for the J $\leftrightarrow$ J' transition.

A new set of selection rules can be derived for J $\leftrightarrow$ J' transitions in lanthanoid ions through assumptions of the Judd-Ofelt theory, as shown in Table 4. However, as an intermediate coupling scheme is assumed for 4f states, S and L cannot be considered as good quantum numbers. Indeed, such calculations are not trivial and may contain large errors. In addition, the Judd-Ofelt theory considers that the (2J + 1)-fold degenerate term sublevels are equally populated, which is not valid at ordinary temperatures according to the Boltzmann distribution.

As a result of such complexities, the Judd-Ofelt theory must be extended in order to account for additional phenomena leading to a further relaxation of selection rules. The initial approach of the Judd-Ofelt theory does not consider the contribution of relativistic effects to lanthanoid

Table 4. Selection rules for transitions between *a* and *b* states of a $4f^n$ configuration according to the Judd-Ofelt theory

	Parity	Spin	Orbital momentum	Total angular momentum
Electric dipole	$\pi_a = -\pi_b$	$\Delta S = 0$	$\Delta L \leq 2\ell$ (≤ 6 for 4f)	$\Delta J \leq 2\ell$ (≤ 6 for 4f) if J or J' = 0, ΔJ = 2, 4, 6
Magnetic dipole	$\pi_a = \pi_b$	$\Delta S = 0, \pm 1$	$\Delta L = 0, \pm 1$	$\Delta J = 0, \pm 1$
Electric quadrupole	$\pi_a = \pi_b$	$\Delta S = 0$	$\Delta L = 0, \pm 1, \pm 2$	$\Delta L = 0, \pm 1, \pm 2$

ions, which, as already mentioned, has prominent effects in their atomic sizes. Readers are referred to a more specific literature for the relativistic approach of the Judd-Ofelt theory.[72,73] Other extensions comprise, for instance, the so-called J-mixing effect.[73-75] In this case, wavefunctions of a $J \neq 0$ state are mixed on a $J = 0$ state through even parity terms of the crystal field. As a result, J is no longer a good quantum number and J-mixing phenomena increase the probability of forbidden $J \leftrightarrow J' = 0 \leftrightarrow 0$ transitions in some symmetries. Another important effect contributing to the relaxation of selection rules is termed dynamic coupling,[76,77] which has been proposed in order to explain the hypersensitivity of some transitions ($\Delta J = 2, 4, 6$) with respect to the chemical environment. This mechanism considers the occurrence of transient local electric dipoles around lanthanoid ions due to the effect of the incident radiation on electrons of ligand atoms, as depicted in Figure 3. In the presence of the dynamic coupling field, the interaction between induced dipoles and quadrupolar transition momenta of central RE^{3+} ions results in a non-zero transition momentum. This effect is obviously dependent on the symmetry of the occupied sites, being forbidden in the presence of an inversion center. In low symmetries, larger the magnitudes of induced electric dipole lead to higher dynamic coupling contributions the total spectral intensity.

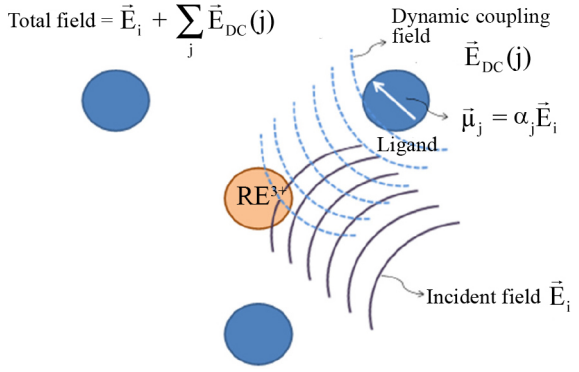

Figure 3. Representation of the dynamic coupling effect in lanthanoid ions. Adapted from reference 77.

3.3. Absorption by Ln^{3+} ions

The description of light absorption by lanthanoid ions involves three main schemes that depend on the nature of the electronic transitions involved. The first comprises intraconfigurational $4f^n$ transitions (Figures 1 and 2), where the effect of the chemical environment on the energy levels is low in comparison to the free ion perturbations. As a result, 4f-4f absorptions are sharp and usually present molar absorption coefficients between < 1 and 10 mol^{-1} L cm^{-1}. Such transitions occur through the forced electric dipole mechanism proposed in the Judd-Ofelt theory, although they can also correspond to magnetic dipole-allowed transitions, which are normally weak. Moreover, 4f-4f absorptions ($\Delta J = 2, 4$) can also display a hypersensitive behavior, presenting intensity alterations higher than 100 times depending on the chemical environment. Such processes are also named as pseudo-quadrupolar transitions.

The second kind of electronic transition commonly observable in lanthanoid ions comprises $4f^n$-$4f^{n-1}$, 5d absorptions, which can occur as broad and highly intense bands. As these transitions are parity- and spin-allowed even in Russell-Saunders coupling selection rules, such processes are associated with very high absorption coefficients and absorption cross sections (ca. 10^{-18}-10^{-17} cm^2).[41] The broad nature of $4f^n$-$4f^{n-1}$, 5d bands arises from very high contributions of 5d states, which are more strongly affected by the chemical environment than 4f states (Figure 4). In this case, large crystal field splitting of $4f^{n-1}$, 5d states can be caused by short metal-ligand distances or by ligands leading to high covalence in chemical bonds. Such ligands comprise electron rich and highly polarizable donor atoms, which are more easily affected by the lanthanoid cations. Although 4f-4f transitions can occur in a wide range of energies from near infrared (NIR) to ultraviolet (UV), $4f^n$-$4f^{n-1}$, 5d transitions usually involve high energy states. As a consequence, $4f^n$-$4f^{n-1}$, 5d absorption bands occur in the UV and vacuum ultraviolet (VUV, $\lambda < 200$ nm) regions. However, Ce^{3+} and Tb^{3+} can present 4f-5d absorptions at lower energies ($\lambda > 300$ nm) depending on the crystal field strength.

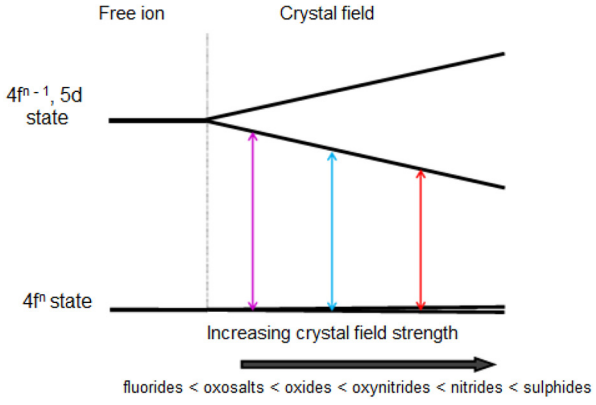

Figure 4. Differences between the crystal field splitting of $4f^n$ and $4f^{n-1}$, 5d states in lanthanoid ions and main classes of compounds related to weak and strong crystal field splitting in RE solid state compounds.

The third type of lanthanoid absorption involves charge transfer (CT) transitions, which are also parity- and spin-allowed and give rise to highly intense broad bands. Such transitions comprise electron transfers from ligands to lanthanoid ions with lower oxidation states at close

energies (ligand-metal charge transfer, LMCT), as well as electron transfers from oxidable lanthanoid species to electron-acceptor ligands (metal-ligand charge transfer, MLCT). LMCT transitions are highly important for a number of RE optical applications, being usually observed in Ce^{4+}, Pr^{4+}, Sm^{3+}, Eu^{3+}, Tb^{4+}, Tm^{3+}, and Yb^{3+} ions in the UV range. MLCT processes are less often observed in lanthanoid ions, with exception of cerium, which has the most stable tetravalent state within the group. As CT and 4f-5d transitions occur in similar wavelengths with comparable intensities, confusions between these two processes are commonly found in articles dealing with the attribution of absorption bands. In addition, confusions of CT processes with resonant energy transfer processes between two different species are even more frequent in the literature, usually as a result of wrong parallels with d-block metal complexes.

3.4. Emission by lanthanoid ions

Emission spectra of $4f^n$ ions involve the same absorption characteristics of lanthanoid ions regarding the nature of the electronic transitions, bandwidths and intensities. With exception of the spectroscopically inert Sc^{3+}, Y^{3+}, La^{3+} and Lu^{3+} ions, the RE ions display luminescent properties ranging from the UV to the NIR region, which can arise from narrow 4f-4f emissions or broad 5d-4f brands. Both emission types have contributions concerning the application of lanthanoids, even though the use of 5d-4f emitters is usually restricted to Ce^{3+} and Eu^{2+}.[40-43] Most of the practical importance associated with lanthanoids is due to their forced electric dipole 4f-4f emissions, which can give rise to very high intensities according to the Ln^{3+} ion and chemical environments.

The emission probability of $4f^n$ excited states can also be described by the Judd-Ofelt theory in terms of Einstein spontaneous emission coefficients (A). Such coefficients are expressed in frequency units (s^{-1}) and indicate the number of spontaneous radiative decay events *per* unit of time. The A coefficients can be determined from forced electric dipole transition strengths between two J ↔ J' manifolds of a 4f configuration through the adjustment of Ω_λ parameters and tabulated matrix elements (equation 5). In this sense, the A coefficients for J ↔ J' $4f^n$ transitions can be expressed as:

$$A(J',J) = \frac{32\pi^3 e^2 \nu^{-3}}{3\hbar(2J'+1)}\left[\frac{n(n^2+2)^2}{9} + D_{ED} + n^3 D_{MD}\right], \quad (5)$$

where ν is the average transition energy in cm^{-1}, ħ is the reduced Planck constant (1.054×10^{-27} erg s^{-1}), and n is the refractive index of the medium. The contribution of magnetic dipole transition strengths (D_{MD}) to the global transition probability is usually low for lanthanoid ions and can be more easily calculated, since this term is practically independent of the chemical environment. Indeed, strength of a magnetic dipole transition is independent of the Ω_λ parameters and can be calculated from equation 6:

$$D_{MD} = \left(\frac{eh}{4\pi m_e c}\right)^2 \left|\langle \Psi' J' \| L + 2S \| \Psi J \rangle\right|^2, \quad (6)$$

where m_e is the electron mass and c is the speed of light. Therefore, the Judd-Ofelt theory also provides the description of $4f^n$ emission spectra in terms of A emission coefficients, which can be related to oscillator strengths and excited state lifetimes. However, due to the approximations of the Judd-Ofelt theory and the need to adjust the Ω_λ parameters, the experimental determination of emission coefficients and lifetimes for the further comparison of chemical environment parameters is more common.

In this sense, the narrow f-f transitions of lanthanoids can attain high intensities, thus making these ions adequate for the generation of the three primary colors in optical devices.[21,41] To this end, Ln^{3+} ions are applied as activators, which means that they are the chemical species actually responsible for the optical properties of the material, being normally added at low concentrations. For instance, emissions of Tb^{3+} ions occur mainly in the green region due to $^5D_{3,4} \rightarrow {}^7F_J$ transitions, in which the $^5D_4 \rightarrow {}^7F_5$ transition at 545 nm is often predominant. This wavelength corresponds to the color of highest sensitivity of the human eye. In addition, the Tb^{3+} level scheme enables a high efficiency of radiative decay, thus making this species a highly advantageous activator for the generation of green light in luminescent materials.[40] Considering other Ln^{3+} ions, this kind of application can be essentially difficult depending on the energy level scheme, which is the case, for instance, of trivalent thulium. Tm^{3+} ions are chemically stable and can present intense blue emissions at ca. 450 nm and ca. 470 nm arising from $^1D_2 \rightarrow {}^3F_4$ and $^1G_4 \rightarrow {}^3H_6$ transitions. However, the complex level structure of Tm^{3+} often results in very low emission intensities in most host lattices as a consequence of competitive emissions in the infrared.

The most widely investigated lanthanoid regarding emission properties is trivalent europium, which also presents the highest commercial importance in the preparation of optical devices. Some Eu^{3+}-based red phosphors as Y_2O_3:Eu^{3+}, Y_2O_2S:Eu^{3+}, and YVO_4:Eu^{3+} were considered inviable and without a commercial future at the time of their development but still today no substitutes with equivalent performance have been found for their

total replacement. Emissions of Eu^{3+} ions consist in a set of lines in the red, being mainly assigned to $^5D_0 \rightarrow {}^7F_J$ (J = 0-6) transitions. In some cases, emissions from high energy levels ($^5D_1$, $^5D_2$, and $^5D_3$) are observable with low intensities, which tend to become lower as the Eu^{3+} concentration in the host lattice increases. Eu^{3+} $^5D_0 \rightarrow {}^7F_J$ transitions display not only a high technologic importance, but also a prominent role in the study of spectral features of lanthanoid ions and 4f-4f transitions. As the $^5D_0$ emitting level is non-degenerate and the final J values are low (J = 0-6), Eu^{3+} electronic spectra are sufficiently simple to allow the attribution of site symmetries occupied by the lanthanoid ion. This is possible because $^5D_0 \rightarrow {}^7F_J$ transitions present a remarkably characteristic unfolding with regard to symmetry sites.[40,41,78] The $^5D_0 \rightarrow {}^7F_0$ transition is particularly important since both initial and final states have J = 0. As a result, each chemical environment occupied by the Eu^{3+} ions is expected to give rise to a maximum of one signal related to the $^5D_0 \rightarrow {}^7F_0$ transition. However, the activity of the $^5D_0 \rightarrow {}^7F_0$ transition is governed by the site symmetry, whereas observed intensities strictly depend on the extent of J-mixing. As a consequence, the presence of a single $^5D_0 \rightarrow {}^7F_0$ signal does not necessarily ensure the occurrence of a single Eu^{3+} site. The Eu^{3+} $^5D_0 \rightarrow {}^7F_1$ transition is allowed by a magnetic dipole mechanism and its intensity is practically independent of the chemical environment. For this reason, the $^5D_0 \rightarrow {}^7F_1$ transition can be used as a reference to the analysis of other Eu^{3+} transitions. The $^5D_0 \rightarrow {}^7F_2$ transition is main origin of the red color of Eu^{3+} emissions. This transition is hypersensitive to the chemical environment, thus being strongly suppressed in the presence of an inversion center. In this sense, the use of a ratio between the intensities of the $^5D_0 \rightarrow {}^7F_2$ and $^5D_0 \rightarrow {}^7F_1$ transitions is common in order to perform comparisons concerning the symmetry of occupied sites. However, the inherent complexity of different Eu^{3+}-containing systems can introduce a number of issues, which make difficult such kinds of comparison. In this context, it is worth mentioning that several considerations regarding the Eu^{3+} emissions also cause a number of misinterpretations regarding a variety of situations of peculiar luminescent systems. In order to avoid them, readers are referred to an elucidative tutorial review.[79]

4. Applications of RE-Based Solid State Materials

4.1. Photoprotection and photocatalysis

Concerning the broad range of applications of RE compounds, the use of lanthanoid absorptions for the development of photoprotective materials capable of selectively attenuating different wavelengths receives increasing attention. In some cases, light absorption can result in the controlled conversion or degradation of organic compounds, which also enables using RE-based materials as photocatalysts. This section is devoted to describing photoprotective and photocatalytic systems based in RE ions, with special attention to the attenuation of UV radiation in biological systems, as well as the possibility to perform sunlight-activated reactions mediated by tailored photocatalysts.

Sunlight that reaches the surface of the Earth contains a broad range of wavelengths from mid infrared to UV.[80-82] Solar radiation is essential to several biochemical processes, such as photosynthesis,[83] color detection by human eyes,[84] synthesis of vitamin D,[85] among others. Solar radiation is also significant in heterogeneous photocatalysis, which was initially developed to produce fuels from cheap materials, aiming at the transformation of solar into chemical energy.[86] Currently, photocatalysis is contextualized in a broader environment of technological development with applications that deal with the degradation of organic substances,[87] anti-bacterial sterilization of medical tools,[88] photodynamic therapy,[89] and to energy conversion processes (solar[18,90] and fuel[91] cells).

UV radiation contained in the sunlight may cause the degradation of materials (photo-oxidation) and change their physical and chemical properties.[46,92,93] Moreover, in extreme cases the UV radiation can lead to sunburn and serious skin damage.[46,81,92,94] Repeated exposures to UVB and UVA solar radiation are the main cause of malignant skin tumors, including melanoma.[95] UV radiation is usually divided and classified into three regions: UVA (320-400 nm), UVB (280-320 nm) and UVC (100-280 nm), which are related to biological effects in human tissue.[93-96]

4.1.1. Rare earth materials for UV protection

The development of materials showing improved performance with stability under long term UV have attracted the attention of the scientific community as well as cosmetic, paints, varnish, plastic and wood manufactures.[96] The main industrial interest in these systems comprises developing and improving sunscreens or filters able to protect efficiently and prevent the degradation of materials when they are exposed to light. Furthermore, inert shields which do not affect the applicability of the protected materials are usually required.

UV-Shielding materials consist of organic or inorganic compounds that act by UV absorbing and/or scattering mechanisms with high transparency in the visible region.[97] Organic filters can cause irritation to the skin, may be

dangerous at high concentration, and may penetrate the skin leading to a decrease in protection efficiency. Organic filters are also limited, due to their sensitivity to heat and self photodegradation leading to a low effective operational lifetime. Inorganic UV-shielding materials, on the other hand, have attracted attention because of advantages such as high solar protection factors, broad spectrum UV protection, and reduced potential irritancy (i.e., cosmetic acceptability).[98]

Among the materials employed as inorganic UV filters, TiO_2 and ZnO are widely studied and used since these oxides have band-gap values compatible with UV radiation and the ability to scatter and/or absorb UV light efficiently.[97] Furthermore, due to the great number of studies involving such materials, they are applied as UV-shielding for different purposes.[99] While their band-gap favors UV absorption, the preparation of particles with suitable sizes can promote light scattering of wavelengths of the same order of magnitude as the particle sizes.[100] Although TiO_2 and ZnO are widely employed in materials protection avoiding the photodegradation, such UV filters show high photocatalytic activity and, when irradiated by UV light, they can induce the formation of reactive oxidizing species, which are generally undesirable.[101]

In this context, considerable attention is focused on RE elements, especially on the cerium-based compounds, which has interesting properties making it a good substitute for zinc or titanium. As above mentioned, cerium shows a [Xe] $4f^15d^16s^2$ electronic configuration (Table 1) and two oxidation states: Ce^{3+} ($4f^1$) and Ce^{4+} ($4f^0$). Ce^{3+} UV absorption properties are based on $^2D \leftarrow {}^2F_{5/2}$ (4f-5d) transitions, while Ce^{4+} absorptions are based on CT transitions. Both processes are spin and parity-allowed transitions, which give rise to broad and intense bands with appreciable UV absorptivity ($> 10^3$ L cm^{-1} mol^{-1}).[102,103] Cerium is the most abundant RE the surface of the Earth (more than copper), being usually found in many minerals, mainly monazite and bastnasite.[104] Due to its high availability, cerium is often studied and has become an interesting element for photoprotective materials.

Throughout the past few decades, a wide scientific interest was devoted to cerium nanoparticles due to their unique characteristics and options for many applications. Cerium-based materials with reduced particle sizes exhibit high absorption in the UV region, low refractive index, high thermal stability, high hardness and reactivity in catalytic applications.[46,101] Moreover, photocatalytic activities of cerium-based materials are usually lower than pure TiO_2 and ZnO, favoring their employment as UV filter.

Ceria nanoparticles (CeO_2) have been the most studied material containing RE for photoprotection and/or UV absorption.[25,26] A wide range of methodologies are employed to obtain materials with ideal particle size, morphology and structure for desirable application. Although ceria shows the ability to absorb UV radiation, initially ceria was not employed in sunscreens, because of its well-known ability to oxidize organic species.[105,106] In the beginning of the 21st century, S. Yabe and his group affirmed that CeO_2 had ideal characteristics to be used as a broad spectrum inorganic sunscreen, because it is transparent to visible light, possess excellent UV absorption properties, and is aesthetically acceptable for cosmetic uses. In two consecutive and important papers, Yabe *et al.*[101,107] have reported the synthesis of pure and doped CeO_2 with UV shielding properties. CeO_2 ultrafine particles doped with M^{2+}/RE^{3+} (Mg^{2+}, Ca^{2+}, Sr^{2+}, Ba^{2+}, Y^{3+}, La^{3+}, Nd^{3+}, Sm^{3+}, Eu^{3+}, Tb^{3+}) were synthesized by a soft chemical route at 40 °C. Among the studied compounds, CeO_2 doped with Zn and Ca (20% mol) have showed best results to reduce the photocatalytic activity of the degradation of castor oil, with excellent UV absorption capability.

In an attempt to improve the absorbing properties of CeO_2 and take advantages of oxides with well-known applications such as ZnO, systems containing ZnO and CeO_2 have been described in recent years using different methodologies like sol-gel,[108] Pechini method,[109] wet-chemical precipitation,[110] soft solution chemical processes,[111] and others. ZnO-CeO_2 nanocomposite systems showed good UV absorption and transparency to visible light without evident decrease in UV absorption. The photocatalytic activity of ZnO-CeO_2 systems for organic compound oxidation is much smaller than observed in titania, ceria, and zinc oxide. Therefore, findings of recent works suggest that the ZnO-CeO_2 systems are promising candidates for use as optical UV-filters even in the presence of organic materials.

Recently, new and interesting applications of CeO_2 UV filters have been reported, such as the protection of natural protein fibers, outdoors, vehicles, and woods. Lu *et al.*[112] have reported the necessity to develop CeO_2 for the protection of a natural protein fiber (silk from *Bombyx mori* cocoons) similar to human skin, which is extensively used by the textile industry. Combination of multifunctional nanomaterials with silk has been regarded as one of the most effective strategies to obtain silk with new properties. Limitations of silk application include microbial adhesion and photoinduced aging. In order to revert such limitations, silver nanoparticles (AgNP) are usually included in the fiber due to their antibacterial nature, which in turn causes silk darkening. CeO_2 nanoparticles immobilized on the surface of silk by dip-coating lead to excellent UV shielding ability and strong antibacterial activity, as indicated by diffuse

reflectance spectroscopy and colony-forming capability test results. Furthermore, the presence of ceria increased the decomposition temperature of the silk suggesting a better thermal stability of the final material.[112]

Coatings containing RE for UV protection have also been widely investigated, since automotive coatings, outdoors, and glasses generally receive a loading of UV absorbers additives or hindered amine light stabilizers (HALS).[113,114] It is known that organic UV absorbers may be converted into radicals, which reduces the UV absorption ability as well as may lead to a rapid degradation of the environment. Since CeO_2 nanoparticles have a suitable band-gap to act in both UVA and UVB regions, crystal defects or impurities can make CeO_2 nanoparticles n-type semiconductors, with band-gaps (E_g) ranging from 2.9 to 3.5 eV depending on the particle size. In addition, mainly in comparison with TiO_2, cerium oxide is able to absorb UV without being photoactive. Saadat-Monfared *et al.*[114] have attributed this effect to the localized electron of cerium oxide (4f orbital) and also to the cerium-oxygen bonding, which is more ionic than the titanium-oxygen bonding, thus the charge carriers (electrons and holes centers) creation is less in the case of titanium oxide. Moreover, they have emphasized that cerium oxide shows faster recombination of charge carriers avoiding the formation of further free radicals. In addition, different amounts of surface-modified nano-ceria suspension were separately added in a water-based polyurethane resin, and clear coats containing CeO_2 have showed better resistance than pure polyurethane film after 700 h UV exposure.[114]

Likewise cosmetic formulations, CeO_2 systems containing zinc oxide have been proposed as clear coats and high UV absorption for automotive, paints, varnishes, glasses, and other applications. The preparation of such systems is reported by different methods, whereas depositions are usually performed by dip-coating, casting and spin-coating techniques.[106] The ideal film band-gaps (ca. 3.1 eV) are correlated to both oxides crystal structures acquired during the syntheses, enabling the application of these films as solar protective coating. The preparation of cerium oxides associated with other RE elements has also been reported. Tessier *et al.*[115,116] described the synthesis and characterization of solid systems containing yttrium and cerium (CeO_2-Y_2O_3) prepared by four different synthesis routes. They have shown the possibility to tune the absorption edge position of ceria by substituting yttrium for cerium atoms. All the reported compositions have displayed strong absorption near 400 nm, and refractive indexes have been estimated about 2.0, which is lower than pure CeO_2 and TiO_2. Furthermore, photocatalytic tests with phenol have showed negative results and these compositions have become interesting UV absorbers for the wood industry.[116]

In contrast, many studies have pointed to the phototoxicity of CeO_2 particles and also that this compound has a non-negligible photocatalytic activity, although reduced compared to commercial oxides (ZnO and TiO_2). In this context, cerium phosphate ($CePO_4$) is a very promising inorganic UV absorber for substitution of the current sunscreen filters. Cerium phosphate presents high UV absorptivity, a lower refractive index than TiO_2 and ZnO, greater chemical inertia, and lower photocatalytic activities. The use of cerium phosphates as UV absorbers in cosmetic applications has been reported, as in the case of cerium and titanium pyrophosphates ($Ce_{1-x}Ti_xP_2O_7$),[117] hydrated cerium phosphate ($Ce_2(PO_4)_2HPO_4.H_2O$)[118] and, $CePO_4$-CeP_2O_7.[119]

Lima and Serra[46] have synthesized and characterized $CePO_4$ nanoparticles with excellent UV protection ability. The intense UV absorption of $CePO_4$, covering mainly the UVA and UVB regions, is due to 4f-5d transitions of Ce^{3+} ions and, a small portion is due to the contribution of valence band to conduction band absorptions. The low transparence in the UV region is influenced by the reduced particle sizes of $CePO_4$ that allow minimal reflection. Lima and Serra[46] have showed that phosphates prepared by modified Pechini, hydrothermal, and microemulsion methods have low diffuse reflectance in the UV region, indicating high UV absorption. The UV protective ability has been evaluated by castor oil photodegradation, and a remarkable reduction in the phtotodegradation in the presence of $CePO_4$ nanoparticles has been observed. These results evidence the application of $CePO_4$ as inorganic UV filters.

4.1.2. Photocatalytic materials: a brief comment

Materials containing RE can also be employed as photocatalysts. In this case, materials that are well developed for photocatalysis, such as anatase-type TiO_2,[120] are doped with any rare earth, although cerium materials comprise the largest number of articles on the subject. Addition of REs to the compounds exhibiting photocatalytic properties leads to a decrease in the material band-gap, expanding the range of light attenuation by shifting the light absorption edge to lower energies. The decrease in the band-gap enhances the light utilization, notably favoring the employment of materials using sunlight instead of artificial lights to have an efficient photocatalysis.[121]

Lima *et al.*[122] have recently published a simple solvothermal synthesis of anatase TiO_2 containing cerium for photocatalytic H_2 generation. The syntheses provided high activity photocatalysts based on large amounts of Ce^{3+} incorporated on polycrystalline titania, which is indispensable for optimal properties. The control of

cerium oxidation state is also crucial for photocatalytic applications, allowing hydrogen production from water.

It is important to mention that several photocatalysts containing RE elements have their mechanisms based on the ability of Ln^{3+} to form complexes with amines, aldehydes, alcohols and related groups. For example, in the photodregadation of Lewis base-type pollutants, the presence of any RE may favor the photocatalyst-pollutant interaction. Additionally, lanthanoid ions can act by increasing the stability of the associated oxide by preventing its segregation.[123]

4.2. Phosphors

4.2.1. Fundamentals of luminescence

The term luminescence was used for the first time by the German physicist Eilhard Wiedemann in 1888 in order to define "all light phenomena that are not conditioned by a temperature increase only".[124] Even though Wiedemann did not have a deep knowledge regarding the structure of matter and its interaction with light, such a definition is still sufficiently wide to provide a good idea about this phenomenon. Currently, the International Union of Pure and Applied Chemistry (IUPAC) Gold Book[125] defines as luminescence the spontaneous emission of electromagnetic radiation by electronically excited species which are not in thermal equilibrium with their environment. This definition thereby excludes incandescence phenomena, which comprise light emission by bodies at high temperatures following the Wien law.

Luminescence phenomena are usually classified according to the nature of the excitation energy, that gives rise to the excited state, as described in Table 5. A more specific classification concerns the selection rules involved in the emission processes (Light Emission and Absorption by Lanthanoid Ions: Basic Aspects section). An emission that is a result of an allowed transition has a high probability to occur, thus being associated with a short-lived emitting state. These phenomena are termed fluorescence, in which the luminescence process involves excited states with short lifetimes ($< 10^{-8}$ s). If the emission arises from a forbidden transition, the emitting state has a low probability of decay and usually displays a long lifetime ($> 10^{-6}$ s), in a process named as phosphorescence. Such classification based in excited state lifetimes is not sufficiently consistent, since these ranges of times are completely dependent on the nature of the observed systems and vary considerably. In addition, excited state lifetimes do not reflect necessarily the nature of electronic transitions, since even a short-lived excited state can give rise to a forbidden transition. Therefore, processes are more rigorously classified according to the spin selection rule for electric dipole transitions.[42] In this sense, the term fluorescence is associated with spin-allowed transitions ($\Delta S = 0$), and phosphorescence with spin-forbidden transitions ($\Delta S \neq 0$). However, as the 4f configurations involve a high number of electronic states and due to the intrinsic mixed nature of the levels, the 4f-4f emission transitions should not be classified as fluorescence or phosphorescence phenomena, being more properly termed simply as luminescence.

The lifetime of excited states involved in the emission processes are usually numerically treated with regard to decay probabilities. In a transition between two levels, the

Table 5. Classification of luminescence phenomena according to the excitation

	Excitation type	Example
Photoluminescence	photons (VUV, UV, Vis, NIR)	quinine, rhodamine, fluorescein, ruby ($Al_2O_3:Cr^{3+}$)
Chemiluminescence	energy of chemical reactions	luminol and H_2O_2
Bioluminescence	chemiluminescence involving biological systems	fireflies (luciferin/luciferase), deep sea animals
Crystalloluminescence	chemiluminescence involving the formation of crystals	crystallization of As_2O_3
Electroluminescence	electric potential difference	lightning strikes, electronic displays
Cathodoluminescence	electron beam	cathode ray tubes
Thermoluminescence	luminescence stimulated by heat (comprises the previous formation of excited states)	chlorophan (a variety of fluorite, CaF_2)
Triboluminescence	mechanic energy, friction	sugar, sodium tartrate
Fractoluminescence	mechanic energy, fracture	ice
Piezoluminescence	mechanic energy, pressure	KBr, KCl
Röntgen- or Radioluminescence	ionizing radiation (X-rays, γ-rays and β-radiation)	$Ba[Pt(CN)_4]$, scintillators
Ionoluminescence	ion or α-particles beam	polar auroras
Sonoluminescence	sound waves leading to the implosion of bubbles in a liquid	water under high power ultrasound

population of the excited state (N_e) is reduced as a function of time (t) according to equation 7:

$$\frac{dN_e}{dt} = -N_e P \quad (7)$$

where P is the probability of spontaneous decay of the excited state, which is related to the nature of the transition and to the chemical environment around the emitting center. Integration of equation 7 yields:

$$N_e(t) = e^{-Pt+C} = e^{-Pt}e^{C}, \quad (8)$$

where C is the integration constant. Therefore, for t = 0, $N_e(t) = e^C$, so that the initial population of the excited state immediately after a pulse ($N_e(0)$) equals e^C. The parameter P corresponds to a probabilistic function that is usually written as $P = \tau^{-1}$. Therefore, equation 8 can be written as:

$$N_e(t) = N_e(0)e^{-t/\tau_R}. \quad (9)$$

The term τ_R is the so-called excited state lifetime, corresponding to the value of t at which the initial population has decayed to 1/e (ca. 37%) of its initial value. Equation 9 illustrates that the depopulation of the excited state in a two level system follows a first order exponential decay. However, if the emitting center occupies different chemical environments, the depopulation can deviate from the monoexponential behavior. The τ_R value is usually accessed through the measurement of the luminescence of a particular excited state as a function of time, since the emission intensity is directly proportional to the population of the excited state. Nevertheless, in complex level structures and systems in which energy transfer processes between excited states take place, the relationship between the population of the emitting state and the emission intensity is not straightforward. In this sense, the measurement of the emission intensity decay potentially gives rise to an "apparent lifetime", for instance: (*i*) in systems in which there is a wavelength superposition between emissions of different states, or (*ii*) in systems where the population of the excited state depends on energy transfer/back-transfer rates.[126]

Another important concept involved in the description of luminescent materials is the energy difference between emission and excitation maxima, which is usually termed Stokes shift. However, the IUPAC Gold Book defines Stokes shift as being "the difference between spectral positions of band maxima of the absorption and luminescence arising from the same electronic transition".[125] The term Stokes shift is therefore limited to situations in which absorption and emission components involve two electronic states, where the vibrational progression of each state gives rise to band broadening and energy differences between the two processes. Such situations occur mostly in organic fluorophores (Figure 5a), in which there is a non-negligible difference between the equilibrium position of ground and excited states ($\Delta R > 0$). Due to the low contribution of 4f orbitals to chemical bonds, energies of ground and excited states of $4f^n$ configurations have practically the same equilibrium position (ΔR ca. 0). As a consequence, a transition between two levels of a $4f^n$ configuration occurs practically without vibrational progression, which virtually gives rise to no shifts between absorption and emission (Figure 5b). A lanthanoid ion can of course be excited in a high energy level of the $4f^n$ configuration at λ_{exc} and, after suitable non-radiative decay to a emitting $^{(2S'+1)}L'_{J'}$ state, it can give rise to a low energy emission with $\lambda_{em} >> \lambda_{exc}$. However, such a process would involve several different electronic states and should not be characterized as a Stokes shift according to the IUPAC definition. In addition, other situations can be pointed out, notably the emission of high energy configurations (such as 5d states, Figure 5c) within the same chromophore, and the emissions arising from antenna sensitizers or charge transfer states (Figure 5d). In the case of 4f-5d transitions in Ln^{3+}, absorption bands consist in a superposition of several electronic transitions that terminate in different states, whereas final states of the emission process are different multiplets of the ground configuration. This process comprises transitions between different sets of crystal field levels, so that it cannot be characterized as a Stokes shift. Recently, it has been suggested to name the energy difference between absorption and emission in these cases as the "Denning shift".[79] Finally, the population of emitting 4f states can be a consequence of a sensitizing action of the chemical environment, such as (*i*) the antenna effect of organic ligands, (*ii*) the sensitizing action of anions (VO_4^{3-}, NbO_4^{3-}, WO_4^{2-}) or cations (Bi^{3+}, Ce^{3+}, Gd^{3+}, etc.), or (*iii*) the occurrence of charge transfer states (for simplicity, only (*i*) is represented in Figure 5d). In these examples, it is more obvious that the differences occur because absorption and emission processes take place in states that originally belong to different chemical species. Such situations were suggested to be termed "Richardson shifts".[79]

Although the loss of the excitation energy through the emission of electromagnetic radiation is the most evident pathway for excited state deactivation and return to the ground state, there are several competing mechanisms acting after the incidence of light by the studied material. These possibilities can both restrict the yield of light emission or reduce the amount of energy that is effectively available for the formation of excited states. In the case of

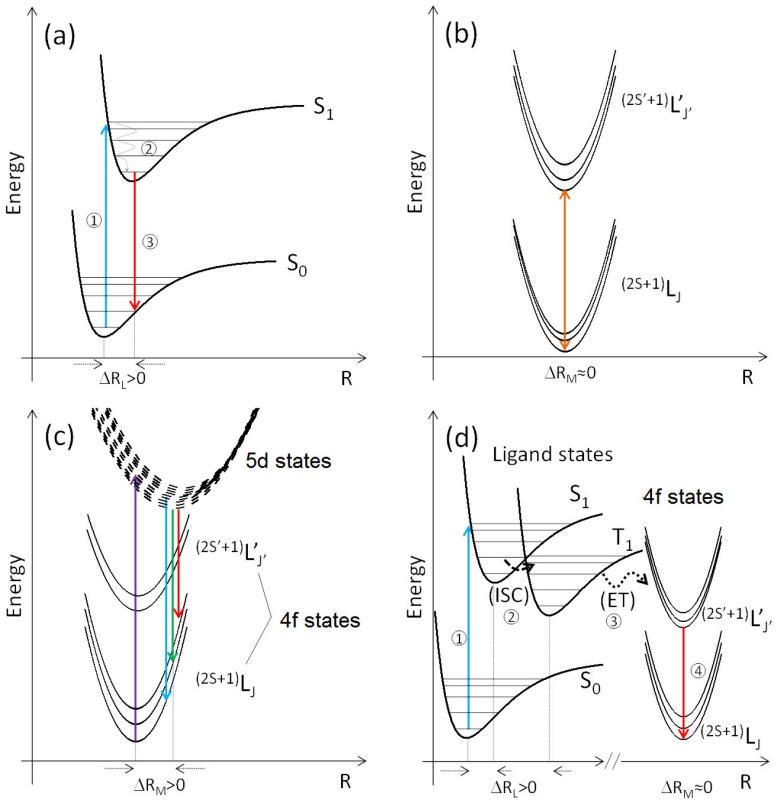

Figure 5. Simplified potential energy diagrams illustrating the origin of shifts between absorption and emission maxima in different situations: (a) Stokes shift in organic fluorophores; (b) pure 4f-4f transition with virtually no shift; (c) "Denning shift", in which absorption and emission processes involve different crystal field states of 4f and 5d configurations of the same chromophore; and (d) "Richardson shift" comprising the energy transfer from ligand excited states to metal levels (antenna effect). S_0: fundamental singlet state; S_1: first excited singlet state; T_1: first triplet state; ISC: intersystem crossing; ET: energy transfer; R; internuclear separation; ΔR: shift in the equilibrium internuclear separation within ligands (ΔR_L) or metal (ΔR_M).

solid state luminescent processes, such mechanisms can be summarized by three situations. For example, if the absorbed energy does not reach the luminescent centers, the emission process will be limited by the generation of the excited states. In a second situation, the absorbed energy reaches luminescent centers, but effective emissions are reduced by the occurrence of non-radiative pathways for the return to the ground state. Finally, in a third situation, the emitted radiation is absorbed by the components of the luminescent material.[40-42] Such processes may occur separately or in combination in luminescent materials, being responsible for luminescence quenching. In the case of lanthanoid ions, concentration quenching mechanisms are particularly important, where the absorbed excitation energy migrates between identical ions in the lattice reducing the probability radiative deactivation. This is the reason why main components in RE-doped phosphors are spectroscopically inert ions, while the activators are present at low concentrations (often < 5% mol/mol). The distance between identical centers become sufficiently small for occurrence of effective energy transfer interactions above a characteristic concentration value, which depends on the nature of the lanthanoid ion and on the lattice properties.[40-42]

For instance, as emission lines in Ln^{3+} ions are often close in energy to absorption lines, the excitation energy of an excited ion can be transferred to a neighboring species. Therefore, the formerly excited ion decays non-radiatively, whereas the neighbor ion is no longer available to absorb the excitation energy, thus reducing the global light generation in the system. This process is known as cross-relaxation, being normally assisted by the absorption or emission of phonons for the compensation of low energy differences between the electronic states. Moreover, high concentrations favor energy migration between identical species, which increases the probability of non-radiative energy loss in impurities or structure defects. However, even at low activator concentrations, the host lattice vibrational structure can also affect emission processes, since vibronic coupling between excited states and high energy oscillators of the lattice can lead to non-radiative decays by means of phonon emission.[40]

Different quenching mechanisms reduce the probability of radiative decays, which culminates in lower luminescence quantum yields. The terms "quantum yield" and "quantum efficiency" are often mentioned as synonyms in the literature of luminescent materials.[42] Despite the lack of

formal conventions that leads to divergent terminologies,[125] authors involved in the description of RE luminescent compounds usually assume that quantum efficiencies and quantum yields represent different quantities. In the present text, we follow the terminologies more often found in the literature of RE compounds, where the quantum efficiency (η) is defined as a ratio of kinetic deactivation parameters (in frequency units) that are particular to each excited state. Therefore, for a given emitting state, the quantum efficiency is defined as the ratio between the Einstein spontaneous emission coefficient (A(J,J') of equation 5, here denoted A_{RAD},) and total decay rate (A_{TOT}), which corresponds to the sum of radiative (A_{RAD}) and non-radiative (A_{NRAD}) decay rates. Therefore, the excited state quantum efficiency becomes:

$$\eta = \frac{A_{RAD}}{A_{TOT}} = \frac{A_{RAD}}{A_{RAD} + A_{NRAD}}. \quad (10)$$

Since, in a given excited state the total decay rate can be considered as the reciprocal of the luminescence lifetime of equation 9, quantum efficiency can also be written as:

$$\eta = A_{RAD}\,\tau \quad (11)$$

Consequently, quantum efficiency is a ratio between decays rates of a particular emitting level of the activator species that lead to a measurable luminescence, thus being independent of the mechanism involved in the formation of the excited state.

The quantum yield (q) is a more global quantity that is associated with the whole system and not only to particular excited states, being defined as the ratio between the photon flux emitted by the system (ϕ_{EM}) and the photon flux absorbed by the system (ϕ_{ABS}):

$$q = \frac{\phi_{EM}}{\phi_{ABS}} \quad (12)$$

where the term ϕ_{EM} may comprise emissions of several excited states. Therefore, quantum yields do not involve the measurement of decay ratios, but the quantification of the number of photons which emerge from the sample instead. This is normally performed by the use of integrating spheres or by comparison with standard compounds with known quantum yield.[127]

Finally, an even wider property can be defined, since not all incident photons are effectively absorbed due to competing events such as transmission, scattering, and reflection. The global emission output that can be provided by the sample is thereby defined as a ratio between the emitted photon flux and the incident photon flux (ϕ_{INC}), which is commonly mentioned as external quantum yield (q_{EXT}) or light output:

$$q_{EXT} = \frac{\phi_{EM}}{\phi_{INC}} \quad (13)$$

In other words, the external quantum yield corresponds to the ratio between the number of photons that are emitted by the sample and the number of photons that reach the sample *per* unit of area *per* unit of time.

4.2.2. RE solid-state phosphors

The use of RE-based solid state phosphors started in the 1960s with the purpose to generate the three primary colors (red, green and blue) in cathode ray tubes and fluorescent lamps. Since then, the evolution and diversification of inorganic phosphors containing RE followed the development of new technologies for lighting and visualization. As a result, RE elements are currently still the most important components in luminescent materials for such applications, as well as several other fields, as detailed in Table 6. Phosphors with practical industrial use are mostly synthesized via high temperature solid-state chemistry techniques, in which simple precursors (e.g., oxides, carbonates, nitrates) are ground together and annealed. Such procedures are normally preferred due to the simple protocols and to the high crystallinity of the final materials. However, the recent advent of particular applications imposing limitations such as high surface areas and low sizes also results in the development of liquid phase synthesis methodologies, which raise a growing importance in different fields.[128]

The development of the final phosphors comprises a delicate balance among several physical and chemical aspects that govern the final efficiency. For instance, solid state luminescent materials usually comprise a spectroscopically inert inorganic host that accommodates chromo- or fluorophore species. Besides this primary role, the inorganic host also must provide a high resistance against (photo)chemical degradation, since high operation lifetimes are usually required, as well as low reactivity in the case of biological applications. In addition, the final emission behavior also depends on the host crystalline structure, since expected spectroscopic properties are governed by site symmetries and covalence provided by the inorganic lattice. In some cases, the host lattice is also expected to generate broad band absorptions, which can be an effective approach to by-pass the low absorptivity associated with RE^{3+} luminescent centers.

In this regard, sensitizing groups are usually related to the design of luminescent materials, since only in a few

Table 6. Some selected properties, applications and compositions of rare earth phosphors

Property	Application	Example	Reference
RGB emission	fluorescent lamps (CFL)	$Y_2O_3:Eu^{3+}$, $LaPO_4:Ce^{3+},Tb^{3+}$, $BaMgAl_{10}O_{17}:Eu^{2+}$,	21-24,40-43
	plasma displays LCD backlighting	$Y(P,V)O_4:Eu^{3+}$, $LaPO_4:Tm^{3+}$, $(Y,Gd)BO_3:Eu^{3+}$,	129-132
	biolabeling	$YVO_4:Eu^{3+}$, $GdVO_4:Eu^{3+}$	133,134
	temperature sensing	$Y_2SiO_5:RE^{3+}$, $Y_3Al_5O_{12}:Sm^{3+}$, $Y_3Al_5O_{12}:Dy^{3+}$	135
Band emission	LED lamps	$Y_3Al_5O_{12}:Ce^{3+}$ $Tb_3Al_5O_{12}:Ce^{3+}$, $SrS:Eu^{2+}$, $CaS:Eu^{2+},Ce^{3+}$ $CaAlSiN_3:Eu^{2+}$, $Sr_2Si_5N_8:Eu^{2+}$	136,137
Persistent luminescence	security, markers	$Y_2SiO_5Eu^{3+}$ $SrAl_2O_4:Eu^{2+},Dy^{3+}$, $Sr_2MgSi_2O_7:Eu^{2+},Dy^{3+}$	138-140
	medical imaging	$(Ca,Zn,Mg)_2Si_2O_6:Eu^{2+},Dy^{3+},Mn^{2+}$ $Zn_{2.94}Ga_{1.96}Ge_2O_{10}:Cr^{3+},Pr^{3+}$	141,142
X-ray excitability	scintillators	$(Lu,Gd)_3Al_5O_{12}:RE^{3+}$ $Gd_2SiO_5:Ce^{3+}$ $LiCaAlF_6:Eu^{2+},Ce^{3+}$	143,144
Upconversion	medical imaging	REF_3, $MREF_4$	145-147
	temperature sensing	$(Pb,La)(Zr,Ti)O_3:Er^{3+}$ $NaYF_4:Yb^{3+},Er^{3+}$ $Yb_3Al_5O_{12}:Er^{3+},Mo^{6+}$, $Yb_3Al_5O_{12}:Tm^{3+},Mo^{6+}$	148-151
	photovoltaics	β-$NaYF_4:Yb^{3+},Er^{3+}$ $LiYF_4:Yb^{3+},Er^{3+}$	17,18,152,153
Downconversion	lighting imaging solar cells	$NaGdF_4:RE^{3+}$	18,154,155

cases are the low molar absorptivity of 4f-4f absorptions sufficiently high to provide useful luminescence yields. The sensitizer characteristics must involve not only a broad and intense absorption, but also the ability to transfer the absorbed energy to emitting groups. This, in turn, refers to the spectral overlap between sensitizer and emitting centers, which depends on a critical distance between the involved species. Such characteristics depend on the volume of unit cells and molar fractions of optically active species, which makes energy transfer parameters mathematically accessible from experimental data.[156-158]

Nevertheless, even if inorganic host and sensitizers provide good general characteristics, the light emission process by a phosphor is completely dependent on the adequacy of the activators regarding desired properties. In this sense, even occurring in low concentrations, activator centers control the major final properties in solid state phosphors. RE ions act as activators in most optical materials, thus being recently termed as the "vitamins of phosphors" by Prof T. Jüstel[159] since, like their biochemical analogues, their presence in low concentrations is indispensable for the operation of the system where they are found, whereas no adequate substitutes are known to perform their functions. The synergism between activators, sensitizers and host thereby governs the final spectroscopic properties and efficiencies, as well as the color associated with the light emitted by the luminescent material. Colorimetry is a crucial subject in the development of phosphors, since color is one of the major limiting aspects for the applicability of luminescent materials. As color is a human perception of chromaticity and brightness rather than a definite physical property, the accurate description of colors associated with emitting compounds is usually considerably complex, and readers are referred to a more specialized literature for further details.[160,161] Color descriptions in the RE phosphors literature are

mostly based on the chromaticity of the emissions, comprising the integration of spectral emission functions with respect to color functions of standard observers, in which the trichromatic (x, y, z) Comission Internationale de l'Eclairage 1931 (CIE 1931) color space is the most often used.[41]

Besides host, sensitizers and activators, the design of solid-state phosphors may also comprise other physicochemical aspects in order to provide the highest adequacy between obtained properties and required applications. For instance, the concentration of structure defects, which can be either intrinsic to the host lattice or introduced through impurities, is also a fundamental characteristic. Defects may induce quenching mechanisms that reduce the global efficiencies or lead to parallel chemical processes that diminish the chemical stability. However, the role of structure defects depends completely on the nature of the luminescent material. For example, characteristic mechanisms and times of persistent luminescence processes are intimately related to defects.[162] In addition, particle morphology and size affect the global efficiency and stability of the luminescent materials, since both light scattering events and surface reactivity are dependent on such parameters. Surface modification on phosphor particles may also play an important role in the study of such compounds, since chemical processes comprising defect passivation, increase of colloidal stability or enhancement of energy transfer efficiencies can be highly important for the final applicability of inorganic solid state phosphors.

In summary, the development of phosphors involves a wide range of chemical (composition, oxidation states, impurity concentration, homogeneity, morphology, particle size, surface charge, etc.) and physical (excitation range, luminescence lifetime, emission color, quantum efficiency, thermal quenching, etc.) aspects, which must be adequately controlled with respect to cost and effectiveness through adequate synthesis methodologies.[40-43]

4.2.3. LED and VUV materials: bright phosphors for a dark future?

The first industrial use of RE phosphors in commercial systems occurred in the 1960s with the introduction of Eu^{3+}-doped compounds as components of fluorescent lamps. At that time, phosphors were mostly broad band emitters such as phosphates ($Sr_3(PO_4)_2$:Sn^{2+}) and halophosphates ($Ca_5(PO_4)_3(F,Cl)$:Sb^{3+},Mn^{2+}). Introduction of the tricolor concept led to the use of more elaborated phosphors, such as Y_2O_3:Eu^{3+}, Y_2O_2S:Eu^{3+}, YVO_4:Eu^{3+}, $LaPO_4$:Ce^{3+}, Tb^{3+} and $Sr_5(PO_4)_3Cl$:Eu^{2+}, which resulted in the improvement of compact fluorescent lamps and cathode ray tubes. However, the increasing development of lighting and visualization technologies and more restrictive energetic and environmental concerns still stimulate the search for a new generation of solid state phosphors. Lighting corresponds to approximately 20% of the total energy consumption in private households.[163] Consequently, future energy policies must mandatorily consider the degree of development of solid state phosphors. For instance, as commercial compact fluorescent lamps (CFL) operate near their technological limit of light output, no large improvements of performance are expected for this class of lamps in the next years. This, in turn, indicates that the other current technologies are potential candidates to bring the next revolution in artificial lighting, which comprises, for instance, light emitting diode (LED) lamps and lighting systems based on VUV phosphors.

Currently, LED lamp devices are the most investigated systems regarding the development of phosphors, since they consist in energetically advantageous solid state lighting sources with potentially improvable output characteristics.[41,136,137,164,165] Yttrium aluminum garnets (YAGs, $Y_3Al_5O_{12}$, Table 6) are the most widely studied class of inorganic compounds for the generation of light in LED systems. YAG solids present a very high chemical stability, as a consequence of their stable complex cubic structure, in which Y^{3+} ions occupy dodecahedral sites and Al^{3+} ions are partitioned between octahedral and tetrahedral sites in a 2:3 ratio. Doping with Ce^{3+} ions leads to the substitution of Y^{3+} ions in dodecahedral sites, thus resulting in a material with high absorptivity in the blue and a broad yellow emission due to Ce^{3+} allowed 5d-4f transitions. The blue light emitted by a LED chip (usually GaN or InGaN) can efficiently excite the yellow luminescence of a YAG:Ce^{3+} solid, whereas the combination of the blue and yellow components generates line-plus-band white light spectrum (Figure 6). This arrangement is significantly efficient in point of view of energy consumption since there is a very low energy loss between excitation and emission, thus making YAG:Ce^{3+} to be referred as an archetypical phosphor for LED lighting due to such possibilities.[163] In addition, the color related to YAG:Ce^{3+} emissions can be efficiently tuned in a wide spectral range (510-590 nm) through the substitution of Y^{3+} by Gd^{3+} or Tb^{3+} and of Al^{3+} by Ga^{3+}, as an effect of the change of ligand field intensities acting on Ce^{3+} levels. An additional advantage of YAG:Ce^{3+} is the short emission lifetime of the Ce^{3+} excited states (10^{-7}-10^{-8} s), which also makes this compound applicable as backlight emitter in displays.[41,136,137]

However, broad band Ce^{3+} emissions do not necessarily lead to final color purities that are adequate to different possible lighting applications, since combination of blue

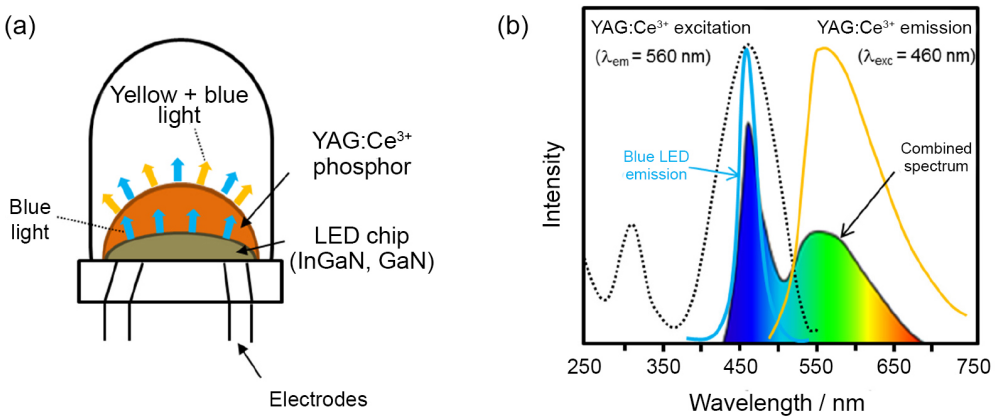

Figure 6. (a) Simplified schematization of a LED bulb and (b) combination of the blue LED spectrum with the YAG:Ce^{3+} emissions to generate a white light spectrum in LED systems.[3,41]

LED emissions with YAG luminescence results in low chromatic stabilities under different currents or different temperatures. The lack of chromaticity is more critical for the red color in YAG:Ce^{3+} emissions. In this sense, other arrangements are studied for the manufacture of LED lamps, such as combinations of (*i*) UV LED and RGB phosphors; (*ii*) blue LED and RG phosphors; and (*iii*) blue LED and red/yellow phosphors. As system (*i*) comprises a complex mixture of phosphors and induces a lower energetic efficiency due to UV excitation, systems (*ii*) and (*iii*) are preferred for the improvement of LED systems, which are currently limited by the lack of an efficient blue light excitable red phosphor. The search for good red phosphors for LED lighting is therefore a highly attractive topic in the RE solid state phosphors research. Eu^{2+}-activated phosphors are particularly important due to the possibility of tuning the broad band Eu^{2+} emissions with alteration of host lattice crystal field parameters. However, as simple oxides do not provide highly intense crystal field splitting (Figure 4), complex compositions with highly polarizable anions, such as nitrides and sulfides, are required to generate red light from Eu^{2+} compounds. For instance, sulfides[166] as CaS:Eu^{2+}, Sr(S,Se):Eu^{2+}, (Sr,Ca)Ga_2S_4:Eu^{2+} and (Y,La)$_2O_2S$:Eu^{3+} are efficient low cost red emitters. However, such compositions are unstable to moisture and they are not adequate to operate in high power LED systems. Moreover, such sulfides react with silver and nickel from electrodes, thus generating the more stable NiS and Ag_2S and the presence of these black compounds decreases the photon flux from the phosphors and reduces the arrangement efficiency. Furthermore, nitrides[167] as $MAlSiN_3$:Eu^{2+} and $M_2Si_5N_8$:Eu^{2+} (M = Ca, Sr, Ba) display excellent luminescent properties under blue light and a very high chemical stability, which is normally only limited by the Eu^{2+}/Eu^{3+} oxidation. However, such compositions have a considerably complex synthesis, in which high purity alkaline-earth metals are usually treated at 1500-2100 °C under high N_2 pressures. As a consequence, the final cost of this kind of phosphor is comparable to pure metallic gold, so that the investigation of new compositions and new synthesis methods are still required for the development of this field.

Despite the mentioned drawbacks, LED systems appear as the most promising technology for a new generation of lighting systems, with some unrivalled advantages such as high efficiency, long operation lifetimes, and emission directionality. However, some particular restrictions can also conduct to a parallel development of other lighting arrangements in order to fulfill specific requirements that can become decisive in the future. For instance, LED bulbs are currently associated with a very high manufacturing cost, even considering final prices *per* lumen (that are decreasing very fast) and high durability.[168,169] Moreover, the concept of LED lamps comprises fundamentally low power devices, which cannot be easily scaled-up as incandescent or fluorescent tubes to provide high power lighting.[168] Additionally, the idea that LED systems are environmentally friendly due to the absence of mercury has been questioned recently, since such devices are associated with a high toxicity potential due to the high levels of arsenic and lead.[170,171] Therefore, the development of new solid state lighting systems must take into account this fact, since the manufacturing of these devices is mainly directed by environmental regulations. For instance, energy consumption restrictions have practically withdrawn low power incandescent lamps from the market in the European Union (2010), USA (2012), and Brazil (2015)[172,173] and future legislations will probably prohibit the use of mercury and other toxic metals in fluorescent and LED lighting systems.

In this sense, VUV phosphors (Table 7) can be considered as potential candidates for the development of

complementary lighting systems that fulfill these specific requirements. This class of luminescent materials involves compounds that are efficiently excited at wavelengths lower than 200 nm, being potentially applicable in combination with noble gas discharges. For instance, xenon and neon are the most used noble gases in discharge mixtures, which can provide exciting radiation at 147 nm (resonant emission line of Xe) plus two continua centered at 152 and 172 nm (molecular emissions of Xe_2) under electric discharge.[174] The application of Xe/Ne plasma as excitation sources for solid state phosphors enabled the development of plasma displays and excimer lamps, which, although not being currently widespread devices, consist in robust technologies that can be widely improved in the future. For instance, since 2014 the principal worldwide manufacturers have abandoned the production of plasma display panels (PDP) due to high production costs and difficult miniaturization of bulky displays, whereas consumers are usually more attracted by thinner arrangements and by the higher brightness of LCD/LED displays, which consist of a cheaper technology. However, PDPs can generally result in larger image sizes as well as faster images (i.e., lower ghosting), thus providing better dark levels and wider vision angles that are more appropriated for the generation of 3D images and for concave displays. Therefore, if new technologies for low cost PDP manufacturing are attained, VUV phosphors with improved efficiency for PDPs will be largely required. The investigation of solid state luminescent materials applicable in such systems still is an essential prospect in this field.

Regarding lighting technologies based on VUV phosphors, excimer lamps present remarkable advantages of temperature independent output, instantaneous operation (i.e., lack of warm up time), and completely arbitrary design, which are characteristics that cannot be found in LED bulbs. In addition, excimer lamps can display very high operation lifetimes (1-5 × 10^5 h) even with high on-off cycles, as a result of the low degradability of the discharge gas in contact with the electrodes. Therefore, VUV phosphors must be continuously improved in order to develop such application field, which can consist in an important technology to complement LED lighting.

VUV phosphors must display some fundamental properties that enable their large scale application, while drawbacks related to currently used materials must be overcome (Table 7). For instance, Eu^{2+} and Mn^{2+}-doped phosphors are susceptible to oxidation processes, which is a problem for long-term utilization. Moreover, some compounds are susceptible to photochemical degradation under VUV irradiation, requiring additional surface coating procedures with MgO or Al_2O_3, for instance. In addition, phosphors with surfaces with high Lewis acidity can lead to the adsorption of excited species of the plasma (such as Xe_2*$^+$), which leads to a lower degree of ground species regeneration (Xe_2/2Xe) as well as efficiency and chromaticity losses due to UVA/B and red light surface reabsorption.[175] The luminescence lifetime of VUV phosphors is also a crucial parameter, mainly for display applications where the number of frames *per* second is a limiting factor during image composition. Emissions that persist for more than 10 ms until intensities are reduced to ca. 10% of initial values are considered long-lived, since they can be detected by the human eye and lead to ghosting in displays. Furthermore, the most fundamental property required of VUV phosphors is a broad and intense absorption band between 147 and 172 nm, which normally is provided by the host lattice. The excitation mechanism in VUV comprises mainly band-gap excitation within the host lattice. This, in turn, results in a very low penetration of VUV radiation (< 100 nm) in solid particles in comparison to UV-Vis (ca. 1-2 μm), which fundamentally concentrates luminescence phenomena under VUV excitation at the particle surface. As a consequence, not only crystallinity and defect density, but also particle size and surface area affect the VUV luminescence efficiency, while nanostructured solids are preferred in order to lead to high luminescence yields. In addition, one of the main drawbacks of VUV phosphors is the very large energy shift between excitation and emission, where a very high fraction of the excitation energy is dissipated in parallel non-radiative processes.

Table 7. Some commercial VUV phosphors and their main current drawbacks

Emission color	Phosphor	Drawback
Blue	$BaMgAl_{10}O_{17}:Eu^{2+}$	Eu^{2+} oxidation
	$CaMgSiO_6:Eu^{2+}$	
	$Y(V,P)O_4$	band emission, temperature dependent
	$LaPO_4:Tm^{3+}$	low brightness, low efficiency
Green	$BaMgAl_{10}O_{17}:Eu^{2+}$, Mn^{2+}	Mn^{2+} oxidation, high luminescence lifetimes
	$(Ba,Sr,Mg)Al_{12}O_{19}:Mn^{2+}$	
	$Zn_2SiO_4:Mn^{2+}$	
	$LaPO_4:Ce^{3+},Tb^{3+}$	Ce^{3+} quenching, high lifetimes
	$(Y,Gd)BO_3:Tb^{3+}$	
Red	$Y_2O_3:Eu^{3+}$	low VUV excitability
	$(Y,Gd)(P,V)O_4:Eu^{3+}$	low band-gap, blue band emission
	$(Y,Gd)BO_3:Eu^{3+}$	orange emission

With the aim to overcome this problem, phosphors with quantum yields greater than unity can be designed based on the so called quantum cutting processes.[41,154,176] In such compounds, each VUV photon generates more than one photon in the visible, thus avoiding the high energy loss associated with low wavelength excitation. This effect is observed in several RE ions, mainly Pr^{3+} and Gd^{3+}/Eu^{3+}, although being usually limited to host lattices with very low vibrational influence on metal states such as fluorides.

5. Conclusions and Outlook

By the end of the 1950s, when the use of Eu^{3+}-doped yttrium oxide was suggested to generate red light in cathode ray tubes and fluorescent lamps, specialists were non-believers about the industrial success of such composition containing two "rare" metals of highly difficult purification. After more than 60 years, no substitutes with equivalent properties have been found for Eu^{3+}-doped compounds, whereas several other RE-activated compounds appeared with a wide variety of unrivalled spectroscopic characteristics. In this sense, RE solid state compounds are completely inseparable from the field of optical materials. The unique properties of this group of elements still stimulates increasing efforts of fundamental and applied research involving lighting, visualization, biolabeling, photoprotection, and photocatalysis, for instance.

Therefore, this text reviewed fundamental concepts concerned in the use of RE-based solid state materials for lighting and photoprotection processes. The elaboration of new applications and the development of tailored properties are completely dependent on a deeper knowledge regarding concepts of 4f spectroscopy. This is particularly important for the development of a new generation of photoprotective materials, with controlled photocatalytic activities and absorptivity, as well as the obtainment of improved energy saving lighting sources. In this regard, investigation of solid state RE materials is crucial for the development of environmentally clean and low energy consumption lighting systems. Furthermore, LED systems comprise the most promising and improvable technology for the next revolution of artificial lighting, whereas the fulfillment of specific environmental and performance requirements (temperature independent output, arbitrary design) also leads to a promising future for lighting systems based on VUV phosphors.

In conclusion, the rare earths are still the friendliest available elements for the construction of new and forthcoming solid state materials for illumination, displays and photoprotection.

Acknowledgements

The authors are grateful to the Brazilian agencies CAPES, CNPq, and FAPESP (Proc. 2013/01669-1 and 2014/22930-2, PCdSF) for financial support.

Paulo Cesar de Sousa Filho *received his BSc (2009) and PhD (2013) degrees in Chemistry from Universidade de São Paulo (FFCLRP-USP) advised by Prof Osvaldo Serra. Currently, he is a post-doctoral researcher in Prof Serra's group in collaboration with Prof Thierry Gacoin at the Laboratory of Physics of Condensed Matter of the École Polytechnique (France). His main research interests concern luminescent and catalytic properties of RE solid-state and coordination compounds, especially the development of new liquid phase synthesis methods and spectroscopic characterization of RE-based nanostructures for applications as lighting phosphors and as active systems for biological probes.*

Juliana Fonseca de Lima *is Assistant Professor at the Departmento de Química Geral e Inorgânica of the Instituto de Química at the Universidade do Estado do Rio de Janeiro since 2015, after receiving her BSc (2009) and PhD (2013) degrees in Chemistry from Universidade de São Paulo (FFCLRP-USP), under direction of Prof Osvaldo Serra, and after a post-doctoral collaboration (2013-2014) at the University of Warwick (United Kingdom) with Prof Richard I. Walton. Her work comprises the development of nanostructured systems for sunlight absorption, UV protection, and photovoltaics through the sol-gel and solvothermal synthesis of cerium, titanium, and zinc compounds.*

Osvaldo Antonio Serra *works in the subject of rare earths since 1961. He is based at the Departmento de Química of the Universidade de São Paulo (FFCLRP) at Ribeirão Preto, Brazil, holding the position of Full Professor since 1983. His research comprises different aspects of RE chemistry, notably new phosphors, nanostructured solids and films for UV absorption, cerium-based catalysts for soot oxidation, and recuperation of RE from domestic and*

industrial waste. Since 2010, he also actively participates of discussions within the Brazilian government for an environmentally sustainable resumption of the exploration and processing of RE elements in Brazil.

References

1. Saez-Puche, R.; Caro, P.; *Rare Earths*; Editorial Complutense: Madrid, 1998.
2. Cotton, S.; *Lanthanide and Actinide Chemistry*; Wiley: Chichester, 2006.
3. Serra, O. A.; Lima, J. F.; de Sousa Filho, P. C.; *Rev. Virtual Quim.* **2015**, *7*, 242.
4. de Sousa Filho, P. C.; Serra, O. A.; *Quim. Nova* **2014**, *37*, 753.
5. Zongsen, Y.; Mimbo, C.; *Rare Earth Elements and Their Applications*; Metallurgical Industry Press: Beijing, 1995.
6. Abrão, A.; *Química e Tecnologia das Terras Raras*; CETEM/CNPq: Rio de Janeiro, 1994.
7. Bünzli, J.-C. G.; Choppin, G. R.; *Lanthanide Probes in Life, Chemical and Earth Sciences*; Elsevier: Amsterdam, 1989.
8. Eliseeva, S. V.; Bünzli, J.-C. G.; *New J. Chem.* **2011**, *35*, 1165.
9. Bünzli, J.-C.G. In *Kirk-Othmer Encyclopedia of Chemical Technology*, John Wiley & Sons, 2013, pp. 1-43. DOI: 10.1002/0471238961.1201142019010.
10. Sastri, V. R.; Bünzli, J.-C. G.; Rao, V. R.; Rayudu, G. V. S.; Perumareddi, J. R.; *Modern Aspects of Rare Earth and Their Complexes*; Elsevier: Amsterdam, 2003.
11. Connelly, N. G.; Damtus, T.; Hartshorn, R. M.; Jutton, A. T.; *Nomenclature of Inorganic Chemistry-IUPAC Recommendations 2005*; RSC Publishing: Cambridge, 2005.
12. IUPAC Periodic Table of the Elements. Available online at http://www.iupac.org/fileadmin/user_upload/news/IUPAC_Periodic_Table-1May13.pdf accessed in November 2015.
13. Alonso, E.; Sherman, A. M.; Wallington, T. J.; Everson, M. P.; Field, F. R.; Roth, R.; Kirchain, R. E.; *Environ. Sci. Technol.* **2012**, *46*, 3406.
14. Massari, S.; Ruberti, M.; *Resour. Policy* **2013**, *38*, 36.
15. Lewism, L. H.; Jiménez-Villacorta, F.; *Metall. Mater. Trans. A* **2013**, *44A*, S2.
16. Poudyal, N.; Liu, J. P.; *J. Phys. D: Appl. Phys.* **2013**, *46*, 043001.
17. Chen, D.; Wang, Y.; Hong, M.; *Nano Energy* **2012**, *1*, 73.
18. Huang, X.; Han, S.; Huang, W.; Liu, X.; *Chem. Soc. Rev.* **2013**, *42*, 173.
19. Ying, T.-K.; Gao, X.-P.; Hu, W.-K.; Wu, F.; Noréus, D.; *Int. J. Hydrogen Energy* **2006**, *31*, 526.
20. Tanaka, T.; Kuzuhara, M.; Watada, M.; Oshitani, M.; *J. Alloys Compd.* **2006**, *408-412*, 323.
21. Jüstel, T.; Möller, S.; Winlker, H.; Adam, W., In *Ullmann's Encyclopedia of Industrial Chemistry*, John Wiley & Sons: Weinheim, Germany, 2012, pp. 1-75. DOI: 10.1002/14356007.a15_519.
22. Feldmann, C.; Jüstel, T.; Ronda, C.; Schmidt, P.; *Adv. Funct. Mater.* **2003**, *13*, 511.
23. Jüstel, T.; *Nanoscale* **2011**, *3*, 1947.
24. Höppe, H. A.; *Angew. Chem., Int. Ed.* **2009**, *48*, 3572.
25. de Sousa Filho, P. C.; Gomes, L. F.; de Oliveira, K. T.; Neri, C. R.; Serra, O. A.; *Appl. Catal., A* **2009**, *360*, 210.
26. Silva, R. F.; de Oliveira, E.; de Sousa Filho, P. C.; Neri, C. R.; Serra, O. A.; *Quim. Nova* **2011**, *34*, 759.
27. Nascimento, L. F.; Martins, R. F.; Silva, R. F.; de Sousa Filho, P. C.; Serra, O. A.; *React. Kinet., Mech. Catal.* **2014**, *111*, 149.
28. Nascimento, L. F.; de Sousa Filho, P. C.; Lima, J. F.; Serra, O. A.; *J. Braz. Chem. Soc.* **2015**, *26*, 1315.
29. Li, F. B.; Li, X. Z.; Ao, C. H.; Lee, S. C.; Hou, M. F.; *Chemosphere* **2005**, *59*, 787.
30. Ranjit, K. T.; Cohen, H.; Willner, I.; Bossmann, S.; Braun, A. M.; *J. Mater. Sci.* **1999**, *34*, 5273.
31. Nieto, A.; Guelly, K.; Kleit, A.; *Resour. Policy* **2013**, *38*, 496.
32. Serra, O. A.; *J. Braz. Chem. Soc.* **2011**, *22*, 811.
33. Binnemans, K.; Jones, P. T.; Blanpain, B.; Gerven, T. V.; Yang, Y.; Walton, A.; Buchert, M.; *J. Cleaner Prod.* **2013**, *51*, 1.
34. Tan, Q.; Li, J.; Zeng, X.; *Crit. Rev. Environ. Sci. Technol.* **2015**, *45*, 749.
35. Hoogerstraete, T. V.; Blanpain, B.; Gerven, T. V.; Binnemans, K.; *RSC Adv.* **2014**, *4*, 64099.
36. Huang, X.-W.; Long, Z.-Q.; Wang, L.-S.; Feng, Z.-Y.; *Rare Met. (Beijing, China)* **2015**, *34*, 215.
37. Migaszewski, Z.; Gałuszka, A.; *Crit. Rev. Environ. Sci. Technol.* **2015**, *45*, 429.
38. Bünzli, J.-C. G.; Comby, S.; Chauvin, A.-S.; Vandevyver, C. D. B.; *J. Rare Earths* **2007**, *25*, 257.
39. Bünzli, J.-C. G.; Eliseeva, S. V.; *Chem. Sci.* **2013**, *4*, 1939.
40. Ronda, C.; *Luminescence: from Theory to Applications*; Wiley: Weinhein, 2008.
41. Yen, W. M.; Shinoya, S.; Yamamoto, H.; *Phosphor Handbook*, 2nd ed.; CRC Press: Boca Raton, 2007.
42. Blasse, G.; Grabmaier, B. C.; *Luminescent Materials*; Springer-Verlag: Berlin, 1994**.**
43. Bünzli, J.-C. G.; Eliseeva, S. V. In *Lanthanide Luminescence: Photophysical, Analytical and Biological Aspects*; Hänninen, P.; Härmä, H., eds.; Springer-Verlag: Berlin-Heidelberg, 2010, pp. 1-45.
44. Shen, J.; Sun, L.-D.; Yan, C.-H.; *Dalton Trans.* **2008**, 5687.
45. Bouzigues, C.; Gacoin, T.; Alexandrou, A.; *ACS Nano* **2011**, *5*, 8488.
46. Lima, J. F.; Serra, O. A.; *Dyes Pigm.* **2013**, *97*, 291.
47. Lima, J. F.; Martins, R. F.; Serra, O. A.; *Opt. Mater.* **2012**, *35*, 56.
48. Gupta, C. K.; Krishnamurthy, N.; *Extractive Metallurgy of Rare Earths*; CRC Press: Boca Raton, 2004.
49. Clark, R.W.; White, G. D.; *J. Chem. Educ.* **2008**, *85*, 497.
50. Jensen, W. B.; *J. Chem. Educ.* **1982**, *59*, 634.

51. Thyssen, P.; Binnemans, K. In *Handbook on the Physics and Chemistry of Rare Earths*; Gschneider Jr., K. A.; Bünzli, J.-C. G.; Pecharsky, V. K., eds.; Elsevier: Amsterdam, 2011, ch. 248, pp. 1-94.
52. Pyykko, P.; *Chem. Rev.* **1988**, *88*, 563.
53. Seth, M.; Dolg, M.; Fulde, P.; Schwerdtfeger, P.; *J. Am. Chem. Soc.* **1995**, *117*, 6597.
54. Wybourne, B. G.; Smentek, L.; *J. Alloys Compd.* **2002**, *341*, 71.
55. Spedding, F. H.; Voigt, A. F.; Gladrow, E. M.; Sleight, N. R.; *J. Am. Chem. Soc.* **1947**, *69*, 2777.
56. Spedding, F. H.; Voigt, A. F.; Gladrow, E. M.; Sleight, N. R.; Powell, J. E.; Wright, J. M.; Butler, T. A.; Figard, P.; *J. Am. Chem. Soc.* **1947**, *69*, 2786.
57. Spedding, F. H.; Fulmer, E. I.; Butler, T. A.; Gladrow, E. M.; Gobush, M.; Porter, P. E.; Powell, J. E.; Wright, J. M.; *J. Am. Chem. Soc.* **1947**, *69*, 2812.
58. Liu, G.; Jacquier, B.; *Spectroscopic Properties of Rare Earths in Optical Materials*; Springer-Verlag: Berlin, 2005.
59. Reisfeld, R. In *Nanostructured and Advanced Materials*; Vaseashta, A.; Dimova-Malinovska, D.; Marshall, J. M., eds.; Springer: Dordrecht, 2005, p.77.
60. van Vleck, J. H.; *J. Phys. Chem.* **1937**, *41*, 67.
61. Judd, B. R.; *Phys. Rev.* **1962**, *127*, 750.
62. Ofelt, G. S.; *J. Chem. Phys.* **1962**, *37*, 511.
63. Smentek, L. In *Computational Methods in Lanthanide and Actinide Chemistry*; Dolg, M., ed.; John Wiley & Sons: Chichester, 2015, ch. 10, pp. 241-268.
64. Smentek, L.; *Mol. Phys.* **2003**, *101*, 893.
65. Wybourne, B. G.; *J. Alloys Compd.* **2004**, *380*, 96.
66. Görller-Walrand, C.; Binnemans, K. In *Handbook on the Physics and Chemistry of Rare Earths*; Gschneider, Jr., K. A.; Eyiring, L., eds.; Elsevier: Amsterdam, 1998, ch. 167, pp. 101-264.
67. Walsh, B. M. In *Advances in Spectroscopy for Lasers and Sensing*; Di Bartolo, B.; Forte, O., eds.; Springer (Online), 2006, pp. 403-433.
68. Racah, G.; *Phys. Rev.* **1942**, *61*, 186.
69. Racah, G.; *Phys. Rev.* **1942**, *62*, 438.
70. Racah, G.; *Phys. Rev.* **1943**, *63*, 367.
71. Racah, G.; *Phys. Rev.* **1949**, *76*, 1352.
72. Smentek, L.; Wybourne, B. G.; Hess, B. A.; *J. Alloys Compd.* **2001**, *323-324*, 645.
73. Lowther, J. E.; *J. Phys. C: Solid State Phys.* **1974**, *7*, 4393.
74. Porcher, P.; Caro, P.; *J. Lumin.* **1980**, *21*, 207.
75. Xia, S.; Chen, Y.; *J. Lumin.* **1985**, *33*, 228.
76. Mason, S. F.; Peacock, R. D.; Stewart, B.; *Chem. Phys. Lett.* **1974**, *29*, 149.
77. Malta, O. L.; Carlos, L. D.; *Quim. Nova* **2003**, *26*, 889.
78. Forsberg, J. H.; *Coord. Chem. Rev.* **1973**, *10*, 195.
79. Tanner, P. A.; *Chem. Soc. Rev.* **2013**, *42*, 5090.
80. De Paula, L. R.; Parussulo, A. L. A.; Araki, K.; Toma, H. E.; *Sens. Actuators, B* **2011**, *156*, 325.
81. Matsumura, Y.; Ananthaswamy, H. N.; *Toxicol. Appl. Pharmacol.* **2004**, *195*, 298.
82. Duffie, J. A.; Beckman, W. A.; *Solar Engineering of Thermal Processes*, 4th ed.; John Wiley & Sons: Hoboken, 2013.
83. Kalyanasundaram, K.; Graetzel, M.; *Curr. Opin. Biotechnol.* **2010**, *21*, 298.
84. Sliney, D. H.; *J. Photochem. Photobiol., B* **2001**, *64*, 166.
85. Sola, Y.; Lorente, J.; Ossó, A.; *J. Photochem. Photobiol., B* **2012**, *117*, 90.
86. Nogueira, R. F. P.; *Quim. Nova* **1998**, *2*, 69.
87. Kuwahara, Y.; Aoyama, J.; Miyakubo, K.; Eguchi, T.; Kamegawa, T.; Mori, K.; Yamashita, H.; *J. Catal.* **2012**, *285*, 223.
88. Maness, P.; Smolinski, S.; Blake, D. M.; Huang, Z.; Wolfrum, E. J.; Jacoby, W. A.; *Appl. Environ. Microbiol.* **1999**, *65*, 4094.
89. Sakai, H.; Baba, R.; Hashimoto, K.; Kubota, Y.; Fujishima, A.; *Chem. Lett.* **1995**, 185.
90. Stathatos, E.; Chen, Y.; Dionysiou, D. D.; *Sol. Energy Mater. Sol. Cells* **2008**, *92*, 1358.
91. Mohammadi, G.; Jahanshahi, M.; Rahimpour, A.; *Int. J. Hydrogen Energy* **2013**, *38*, 9387.
92. Andrady, A. L.; Hamid, S. H.; Hu, X.; Torikai, A.; *J. Photochem. Photobiol., B* **1998**, *46*, 96.
93. Zayat, M.; Garcia-Parejo, P.; Levy, D.; *Chem. Soc. Rev.* **2007**, *36*, 1270.
94. Kockler, J.; Oelgemöller, M.; Robertson, S.; Glass, B. D.; *J. Photochem. Photobiol., C* **2012**, *13*, 91.
95. Rastogi, S. C.; *Contact Dermatitis* **2002**, *46*, 348.
96. Parejo, P. G.; Zayat, M.; Levy, D.; *J. Mater. Chem.* **2006**, *16*, 2165.
97. Serpone, N.; Dondi, D.; Albini, A.; *Inorg. Chim. Acta* **2007**, *360*, 794.
98. Dransfield, G. P.; *Radiat. Prot. Dosim.* **2000**, *91*, 271.
99. Livraghi, S.; Corazzari, I.; Paganini, M. C.; Ceccone, G.; Giamello, E.; Fubini, B.; Fenoglio, I.; *Chem. Commun.* **2010**, *46*, 8478.
100. Flor, J.; Davolos, M. R.; Correa, M. A.; *Quim. Nova* **2007**, *30*, 153.
101. Yabe, S.; Yamashita, M.; Momose, S.; Tahira, K.; Yoshida, S.; Li, R.; Yin, S.; Sato, T.; *Int. J. Inorg. Mater.* **2001**, *3*, 1003.
102. Trovarelli, A.; *Catalysis by Ceria and Related Materials*, 1st ed.; Imperial College Press: London, 2002.
103. Ebendorff-Heidepriem, H.; Ehrt, D.; *Opt. Mater.* **2000**, *15*, 7.
104. Greenwood, N. N.; Earnshw, A.; *Chemistry of the Elements*, 2nd ed.; Butterworth-Heinemann: Oxford, 1997.
105. Balzer, R.; Probst, L. F. D.; Drago, V.; Schreiner, W. H.; Fajardo, H. V.; *Braz. J. Chem. Eng.* **2014**, *31*, 757.
106. Vivier, L.; Duprez, D.; *ChemSusChem* **2010**, *3*, 654.
107. Yabe, S.; *J. Solid State Chem.* **2003**, *171*, 7.
108. Lima, J. F.; Martins, R. F.; Neri, C. R.; Serra, O. A.; *Appl. Surf. Sci.* **2009**, *255*, 9006.

109. Peverari, C.; Pires, A. M.; Gonçalves, R. R.; Serra, O. A.; *Ecletica Quim.* **2005**, *30*, 59.
110. Liu, I.-T.; Hon, M.-H.; Teoh, L. G.; *Ceram. Int.* **2014**, *40*, 4019.
111. Li, R.; *Solid State Ionics* **2002**, *151*, 235.
112. Lu, Z.; Mao, C.; Meng, M.; Liu, S.; Tian, Y.; Yu, L.; Sun, B.; Li, C. M.; *J. Colloid Interface Sci.* **2014**, *435*, 8.
113. You, B.; Zhou, D.; Yang, F.; Ren, X.; *Colloids Surf., A* **2011**, *392*, 365.
114. Saadat-Monfared, A.; Mohseni, M.; Tabatabaei, M. H.; *Colloids Surf., A* **2012**, *408*, 64.
115. Cheviré, F.; Muñoz, F.; Baker, C. F.; Tessier, F.; Larcher, O.; Boujday, S.; Colbeau-Justin, C.; Marchand, R.; *J. Solid State Chem.* **2006**, *179*, 3184.
116. Tessier, F.; Cheviré, F.; Muñoz, F.; Merdrignac-Conanec, O.; Marchand, R.; Bouchard, M.; Colbeau-Justin, C.; *J. Solid State Chem.* **2008**, *181*, 1204.
117. Imanaka, N.; Masui, T.; Hirai, H.; Adachi, G.; *Chem. Mater.* **2003**, *15*, 2289.
118. Sato, T.; Saito, M.; Sato, C.; Yin, S.; *Funct. Mater. Lett.* **2009**, *2*, 157.
119. Cavalcante, P. M. T.; Dondi, M.; Guarini, G.; Raimondo, M.; Baldi, G.; *Dyes Pigm.* **2009**, *80*, 226.
120. Ni, M.; Leung, M. K. H.; Leung, D. Y. C.; Sumathy, K.; *Renewable Sustainable Energy Rev.* **2007**, *11*, 401.
121. Muñoz-Batista, M. J.; de los Milagros Ballari, M.; Kubacka, A.; Cassano, A. E.; Alfano, O. M.; Fernández-García, M.; *Chem. Eng. J.* **2014**, *255*, 297.
122. Lima, J. F.; Harunsani, M. H.; Martin, D. J.; Kong, D.; Dunne, P. W.; Gianolio, D.; Kashtiban, R. J.; Sloan, J.; Serra, O. A.; Tang, J.; Walton, R. I.; *J. Mater. Chem. A* **2015**, *3*, 9890.
123. Jiang, H.; Yan, P.; Wang, Q.; Zang, S.; Li, J.; Wang, Q.; *Chem. Eng. J.* **2013**, *215-216*, 348.
124. Harvey, E. N.; *A History of Luminescence: from the Earliest Times Until 1900*; The American Philosophical Society: Philadelphia, 1957.
125. McNaught, A. D.; Wilkinson, A.; *IUPAC Compendium of Chemical Terminology ("Gold Book")*, 2nd ed. (online); Blackwell Scientific Publications: Oxford, 2006. Available at http://goldbook.iupac.org accessed in November 2015.
126. Carlos, L. D.; Faustino, W. M.; Malta, O. L.; *J. Braz. Chem. Soc.* **2008**, *19*, 299.
127. de Sa, G. F.; Malta, O. L.; Donega, C. M.; Simas, A. M.; Longo, R. L.; Santa-Cruz, P. A.; da Silva, Jr., E. F.; *Coord. Chem. Rev.* **2000**, *196*, 165.
128. de Sousa Filho, P. C.; Serra, O. A.; *Quim. Nova* **2015**, *38*, 679.
129. Batista, J. C.; de Sousa Filho, P. C.; Serra, O. A.; *Dalton Trans.* **2012**, *41*, 6310.
130. de Sousa Filho, P. C.; Serra, O. A.; *J. Phys. Chem. C* **2011**, *115*, 636.
131. Rao, R. P.; *J. Lumin.* **2005**, *113*, 271.
132. Moine, B.; Bizarri, G.; *Mater. Sci. Eng., B* **2003**, *105*, 2.
133. Casanova, D.; Bouzigues, C.; Nguyên, T.-L.; Ramodiharilafy, R. O.; Bouzhir-Sima, L.; Gacoin, T.; Boilot, J.-P.; Tharaux, P.-L.; Alexandrou, A.; *Nat. Nanotechnol.* **2009**, *4*, 581.
134. Abdesselem, M.; Schoeffel, M.; Maurin, I.; Ramodiharilafy, R.; Gwennhael, A.; Clément, O.; Tharaux, P.-L.; Boilot, J.-P.; Gacoin, T.; Bouzigues, C.; Alexandrou, A.; *ACS Nano* **2014**, *8*, 11126.
135. Chambers, M. D.; Clarke, D. R.; *Annu. Rev. Mater. Res.* **2009**, *39*, 325.
136. Ye, S.; Xiao, F.; Pan, Y. X.; Ma, Y. Y.; Zhang, Q. Y.; *Mater. Sci. Eng., R* **2010**, *71*, 1.
137. Smet, P. F.; Parmentier, A. B.; Poelman, D.; *J. Electrochem. Soc.* **2011**, *158*, R37.
138. Hölsä, J.; Laamanen, T.; Lastusaari, M.; Malkamäki, M.; Novak, P.; *J. Lumin.* **2009**, *129*, 1606.
139. Brito, H. F.; Hölsä, J.; Laamanen, T.; Lastusaari, M.; Malkamäki, M.; Rodrigues, L. C. V.; *Opt. Mater. Express* **2012**, *2*, 371.
140. van den Eeckhout, K.; Smet, P. F.; Poelman, D.; *Materials* **2010**, *3*, 2537.
141. Abdukayum, A.; Chen, J.-T.; Zhao, Q.; Yan, X.-P.; *J. Am. Chem. Soc.* **2013**, *135*, 14125.
142. Maldiney, T.; Richard, C.; Seguin, J.; Wattier, N.; Bessodes, M.; Scherman, D.; *ACS Nano* **2011**, *5*, 854.
143. Yanagida, T.; *Opt. Mater.* **2013**, *35*, 1987.
144. Li, G.-J.; Sakka, Y.; *Sci. Technol. Adv. Mater.* **2015**, *16*, 014902.
145. Hao, S.; Chen, G.; Yang, C.; *Theranostics* **2013**, *3*, 331.
146. Chen, Z.; Zheng, W.; Huang, P.; Tu, D.; Zhou, S.; Huang, M.; Chen, X.; *Nanoscale* **2015**, *7*, 4274.
147. Shen, J.; Sun, L.-D.; Yan, C.-H.; *Dalton Trans.* **2008**, 5687.
148. de Camargo, A. S. S.; Possatto, J. F.; Nunes, L. A. O.; Botero, E. R.; Adreeta, E. R. M.; Garcia, D.; Eiras, J. A.; *Solid State Commun.* **2006**, *137*, 1.
149. Vetrone, F.; Naccache, R.; Zamarron, A.; de la Fuente, A. J.; Sanz-Rodrigues, F.; Maestro, L. M.; Rodriguez, L. M.; Jaque, D.; Solé, J. G.; Capobianco, J. A.; *ACS Nano* **2010**, *4*, 3254.
150. Dong, B.; Cao, B.; He, Y.; Liu, Z.; Li, Z.; Feng, Z.; *Adv. Mater.* **2012**, *24*, 1987.
151. Tsang, M.-K.; Bai, G.; Hao, J.; *Chem. Soc. Rev.* **2015**, *44*, 1585.
152. Goldschmidt, J. C.; Fischer, S.; *Adv. Opt. Mater.* **2015**, *3*, 510.
153. Yang, W.; Li, X.; Chi, D.; Zhang, H.; Liu, X.; *Nanotechnology* **2014**, *25*, 482001.
154. Zhang, Q. Y.; Huang, X. Y.; *Prog. Mater. Sci.* **2010**, *55*, 353.
155. Chen, G.; Ohulchanskyy, T. Y.; Liu, S.; Law, W.-C.; Wu, F.; Swihart, M. T.; Agren, H.; Prasad, P. N.; *ACS Nano* **2012**, *6*, 2969.
156. Dexter, D. L.; *J. Chem. Phys.* **1954**, *22*, 1063.
157. Reisfeld, R.; Greenberg, E.; Velapoldi, R.; Barnett, B.; *J. Chem. Phys.* **1972**, *56*, 1698.
158. Zhang, J.; He, Y.; Qiu, Z.; Zhang, W.; Zhou, W.; Yu, L.; Lian, S.; *Dalton Trans.* **2014**, *43*, 18134.

159. https://www.fh-muenster.de/fb1/downloads/personal/juestel/juestel/Rare_Earth-The_Vitamins_of_Phosphors_Juestel_PGS_____2012_.pdf, accessed in November 2015.
160. Luo, M. R.; *Color. Technol.* **2011**, *127*, 75.
161. Wyszecki, G.; Stiles, W. S.; *Color Science: Concepts and Methods, Quantitative Data and Formulae*, 2nd ed.; John Wiley & Sons: New York, 2000.
162. Aitasalo, T.; Dereń, P.; Hölsä, J.; Jungner, H.; Krupa, J.-C.; Lastusaari, M.; Legendziewicz, J.; Niittykoski, J.; Stręk, W.; *J. Solid State Chem.* **2003**, *171*, 114.
163. Meyer, J.; Tappe, F.; Schmidt, N.; *ChemViews Magazine*, DOI: 10.1002/chemv.201500033, available at http://www.chemistryviews.org/details/ezine/7897011/The_Future_of_Lighting.html accessed in November 2015.
164. Shang, M.; Li, G.; Geng, D.; Yang, D.; Kang, X.; Zhang, Y.; Lian, H.; Lin, J.; *J. Phys. Chem. C* **2012**, *116*, 10222.
165. Revaux, A.; Dantelle, G.; Decanini, D.; Haghiri-Gosnet, A.-M.; Gacoin, T.; Boilot, J.-P.; *Opt. Mater.* **2011**, *33*, 1124.
166. Jabbarov, R.; Musayeva, N.; Scholz, F.; Wunderer, T.; Turkin, A. N.; Shirokov, S. S.; Yunovich, A. E.; *Phys. Status Solidi A* **2009**, *206*, 287.
167. Li, J.; Watanabe, T.; Wada, H.; Setoyama, T.; Yoshimura, M.; *Chem. Mater.* **2007**, *19*, 3592.
168. Schubert, E. F.; *Light-Emitting Diodes*; Cambridge University Press: Cambridge, 2003.
169. Wendt, M.; Andriesse, J.-W.; *Proc. IEEE Ind. Appl. Soc. (IAS)* **2006**, *1-5*, 2601. DOI: 10.1109/IAS.2006.256905.
170. Lim, S.-R.; Kang, D.; Ogunseitan, O. A.; Schoenung, J. M.; *Environ. Sci. Technol.* **2011**, *45*, 320.
171. Lim, S.-R.; Kang, D.; Ogunseitan, O. A.; Schoenung, J. M.; *Environ. Sci. Technol.* **2013**, *47*, 1040.
172. Khan, N.; Abas, N.; *Renewable Sustainable Energy Rev.* **2011**, *15*, 296
173. http://www.brasil.gov.br/infraestrutura/2015/07/lampada-incandescente-de-60-watts-sai-do-mercado accessed in November 2015.
174. Maeda, M.; Uchiike, H.; Shinoda, T. In *Handbook of Optoelectronics*; Brown, R. G. W.; Dakin, J. P., eds.; CRC Press: Boca Raton, 2006.
175. Stein, L.; Henderson, W. W.; *J. Am. Chem. Soc.* **1980**, *102*, 2856.
176. Wegh, R. T.; Donker, H.; Oskam, K. D.; Meijerink, A.; *J. Lumin.* **1999**, *82*, 93.

Submitted: August 12, 2015
Published online: November 24, 2015

FAPESP has sponsored the publication of this article.